EPRI | ELECTRIC POWER RESEARCH INSTITUTE

Comparison of American Petroleum Institute 579/American Society of Mechanical Engineers Fitness-for-Service 1 with EPRI Life Assessment Guidelines

Comparison of American Petroleum Institute 579/American Society of Mechanical Engineers Fitness-for-Service 1 with Remaining Life Simulation and Monitoring and Boiler Life Extension and Simulation System

1018999

Comparison of American Petroleum Institute 579/American Society of Mechanical Engineers Fitness-for-Service 1 with EPRI Life Assessment Guidelines

Comparison of American Petroleum Institute 579/American Society of Mechanical Engineers Fitness-for-Service 1 with Remaining Life Simulation and Monitoring and Boiler Life Extension and Simulation System

1018999

Technical Update, August 2010

EPRI Project Manager

K. Coleman

ELECTRIC POWER RESEARCH INSTITUTE
3420 Hillview Avenue, Palo Alto, California 94304-1338 ▪ PO Box 10412, Palo Alto, California 94303-0813 ▪ USA
800.313.3774 ▪ 650.855.2121 ▪ askepri@epri.com ▪ www.epri.com

DISCLAIMER OF WARRANTIES AND LIMITATION OF LIABILITIES

THE FOLLOWING ORGANIZATION, UNDER CONTRACT TO EPRI, PREPARED THIS REPORT:

Becht Engineering Co., Inc.

This is an EPRI Technical Update report. A Technical Update report is intended as an informal report of continuing research, a meeting, or a topical study. It is not a final EPRI technical report.

NOTE

For further information about EPRI, call the EPRI Customer Assistance Center at 800.313.3774 or e-mail askepri@epri.com.

ACKNOWLEDGMENTS

The following organization, under contract to the Electric Power Research Institute (EPRI), prepared this report:

Becht Engineering Co., Inc.
22 Church Street
Liberty Corner, NJ 07938

Principal Investigator
I. Chant

This report describes research sponsored by EPRI.

This publication is a corporate document that should be cited in the literature in the following manner:

Comparison of American Petroleum Institute 579/American Society of Mechanical Engineers Fitness-for-Service 1 with EPRI Life Assessment Guidelines: Comparison of American Petroleum Institute 579/American Society of Mechanical Engineers Fitness-for-Service 1 with Remaining Life Simulation and Monitoring and Boiler Life Extension and Simulation System. EPRI, Palo Alto, CA: 2010. 1018999.

ABSTRACT

The American Society of Mechanical Engineers (ASME) governs the design and construction of power boilers and piping systems in the United States and many other countries. The ASME rules generally cover only the design and construction of these components, whereas rules for maintenance, repair, and life assessment are not addressed. Recently, ASME has been developing guidelines for post-construction activities, including damage assessment and life prediction.

The Electric Power Research Institute (EPRI) has developed many guidelines and software applications to assist utilities in determining if their high-energy components are currently safe to run and how long they can be expected to last. To assist in this effort, EPRI has developed the Boiler Life Extension and Simulation System (BLESS), Prediction of Damage in Service (PODIS), and Remaining Life Simulation and Monitoring (RLSM) software to address degradation of components along with many printed documents with instructions on how to perform life assessment and damage calculations.

Unfortunately, these products are available only to EPRI members, so when ASME was developing its post-construction guidelines, requirements that the information be available publicly required them to look elsewhere for life assessment guidance. ASME adopted methods currently used by the American Petroleum Institute (API) for methods to address damage assessment. This report compares the methods developed by EPRI with API methods accepted by ASME.

Keywords

American Society of Mechanical Engineers (ASME)
Post-construction guidelines
Life assessment
Damage calculations
Creep fatigue

CONTENTS

1
EXECUTIVE SUMMARY

Boiler tube failures are the leading cause of fossil plant downtime worldwide, whereas failures in high-energy piping systems pose significant safety and availability risks. Advances in life assessment modeling tools could improve fossil plant reliability while minimizing maintenance costs by improving the timing of inspection, repair, and replacement activities. The current creep methodology comparison study was carried out to better understand the remaining life predictions produced by the EPRI software programs Remaining Life Simulation and Monitoring (RLSM) and Boiler Life Extension and Simulation System (BLESS) and to compare those methods and results with the American Petroleum Institute (API) 579-1/American Society of Mechanical Engineers (ASME) Fitness-For-Service (FFS) 1, 2007 Edition, model [1]. The types of damage considered in this study include creep rupture, creep fatigue, and creep crack growth.

The Materials Properties Council (MPC) Omega method, which models tertiary creep, was first incorporated into API 579-1/ASME FFS-1 in the 2007 Edition and is presented in the Standard as the preferred approach. API 579-1/ASME FFS-1, 2007, also provides the Larson Miller Parameter (LMP) data as an alternative to Omega for creep rupture evaluation. In addition, it is very difficult to perform a creep crack growth evaluation according to API 579-1/ASME FFS-1, 2007 without using the Omega equations.

RLSM and BLESS have many features in common with the modeling approaches in API 579-1/ASME FFS-1, the main exception being the absence of the Omega model in the EPRI software programs. Because of this, one emphasis of this project has been to present the Omega model and contrast it with the legacy approach, the LMP model.

The Omega and LMP models use different formats and fundamental theoretical bases. RLSM uses an LMP parameter in estimating the time to rupture. The LMP form in RLSM differs from that in API 579/ASME FFS, but the approach and results are fundamentally the same.

The examples prepared considered the materials 2-¼ Cr–1 Mo and 9 Cr–1 Mo in the temperature range of 900°F–1100°F (482°C–593°C). The creep stress levels were maintained below the ASME Section II, Part D allowable stresses.

The Omega and LMP models produce different life predictions. In some cases, the difference is quite large, and the regions of discrepancy for the cases studied are described. Table 1-1 gives a top-level overview of the creep modeling methods evaluated.

An important consideration for accurately calculating creep time to rupture is stress relaxation. This mechanism involves a relaxation of secondary stress as elastic strain is replaced by creep strain that develops. The Omega model can be used to model this relaxation because it provides a model for determining the creep strain rate as a function of accumulated damage. The version of RLSM that was investigated did not have the ability to model stress relaxation, which could lead to excessive conservatism. The user of the program can input a relaxed stress state, but it is not clear how they are to determine this. If the initial stress is used for the relaxed stress, the result

can be very conservative. Structural Integrity Associates (SIA) has indicated that they recently have added the capability to model relaxation [2] in RLSM Any model that includes stress relaxation will have to distinguish between primary and secondary stresses and only relax the proper stresses (that is, the secondary stresses).

RLSM uses a user-defined transfer function to relate pressure and temperature to stress. RLSM states that the transfer function should be based on the ASME B31.1 piping stress analysis report for the subject system. As such, the implication is that the stresses to be used are longitudinal stresses due to thermal expansion. However, the user could use the transfer function to calculate an effective stress considering the multi-dimensional stress state if those stresses were available. However, piping stress analysis results do not provide the appropriate stress information to do such a calculation.

For the BLESS comparison, data sources referenced by BLESS were reviewed in performing fatigue crack growth and creep crack growth to assist in recreating these calculations. The project team was able to benchmark the fatigue and creep components of da/dt using the papers that BLESS references as its basis. There was a slight discrepancy in the stress basis of BLESS when compared with its source publications. Additionally, the project team found a significant difference between the crack depth, a, over time versus the reported da/dt for the fatigue comparison, where the creep coefficient was set exceptionally low in order to focus on fatigue. Comparisons with API 579/ASME FFS predictions were made, and the reasons for discrepancies found are described. Table 1-2 provides a top-level overview of the BLESS model.

Table 1-1
Overview of Major Features of RLSM and API 579-1/ASME FFS-1, 2007 Edition, Sections 10.5.2 and 10.5.3

	RLSM	API 579-1/ASME FFS-1 2007 Edition
Creep rupture life evaluation	Overview: • LMP approach • Single stress considered, based on user input of transfer function • Transfer functions used to scale stresses • Time fraction approach to creep damage	Overview: • Omega model is preferred approach • Average and minimum LMP models also published • Multi-dimensional stress states considered • Time fraction approach to creep damage
	Pros: • Flexible modeling approach as input deck includes user-entered polynomial coefficients	Pros: • Contains material model data for a wide range of materials and conditions • Provides creep strain rate information that can be used for creep relaxation calculations
	Cons: • Does not consider multidimensional stress states • Does not specify whether average or minimum creep rupture properties should be used, although the creep rupture data in the example problem imply average • Does not include Omega model data	Cons: • Some significant differences in time to rupture when LMP and Omega are compared at some combinations of stress and temperature. • Omega model in need of further review for anomalies. • Requires consideration of multi-dimensional stress state and relaxed stress state information, which is not available from piping stress analysis results
Fatigue life evaluation	Overview: • User-supplied fatigue (stress amplitude versus fatigue life) interpolation table • Fatigue damage per load cycle is 1 / cycles to failure • Uses principal stress (although effective stress could be implemented via the transfer function) • Some "rounding up" of stress amplitude makes fatigue damage slightly higher	Overview: • Tables or curves fit to ASME data to correlate stress amplitude (low temperature) or strain range (high temperature) to fatigue life. • Uses effective stress • Fatigue damage per load cycle is 1 / cycles to failure
	Pros: • Flexible user-entered fatigue data	Pros: • Annex F of Standard provides a wide range of fatigue data, including curve

		fits for high-temperature data
	Cons: • User must convert strain ranges to stress amplitude for input deck.	Cons: • Uses effective stress which requires information not typically available from ASME B31.1 stress analysis reports. However, the user could simply use the maximum principal stress.
Creep-fatigue interaction model	Overview: • User-entered damage at failure criterion is sum of creep damage and fatigue damage • Separate fatigue and creep stress states and transfer functions • Incorrectly uses linear combination of creep and fatigue damage for failure criteria	Overview: • Uses nonlinear failure envelope criteria to predict failure. • Separate fatigue and creep stress states can be modeled.
Stress relaxation	Overview: • Not part of evaluated version of RLSM	Overview: • Can be implemented when integrating the operating history, but separate analysis and special programming is required.

Table 1-2
Overview of Major Features of BLESS and API 579-1/ASME FFS-1, 2007 Edition, Sections 10.5.4

	BLESS	API 579-1/ASME FFS-1 2007 Edition
Fatigue crack growth	Overview: • Paris Law Approach • Stress intensity factor expressions from various cited literature sources, dependent on crack and component geometry. • Stress intensity factor uses explicit expression • Failure based solely on user-specified percent of wall penetration by crack	Overview: • Various crack growth models are presented in Annex F • Stress intensity factor based on Annex C correlations or weight function approach [15] • Failure based on crack reaching 80% of wall thickness, operation outside of failure assessment diagram (FAD) envelope or 80% accumulated damage limit
	Cons: • Does not consider multidimensional stress states • Failure does not consider FAD envelope or accumulated damage	Pros: • Allows multidimensional stress states • Failure considers FAD envelope and accumulated damage • Considers stress profiles in wall
Creep crack growth	Overview: • Paris-law type equation used to model time-based creep crack growth	Overview: • Paris-law type equations model time-based creep crack growth. • Omega model is the recommended approach. Creep crack driving force and crack growth rate presented in terms of Omega model • Failure based on crack reaching 80% of wall thickness, operation outside of FAD envelope or 80% accumulated damage limit
	Cons: • Does not incorporate Omega material model. • Failure criteria do not include FAD or accumulated damage • Does not consider multidimensional stress state • Does not consider finite element analysis (FEA) (or other) derived stress profile.	Pros: • Annex F of Standard provides a range of crack growth models, including high-temperature operation • Allows multidimensional stress state • Allows consideration of FEA derived (or other) stress profile

2
INTRODUCTION

This report documents the findings of a study undertaken to perform a review of creep rupture, creep-fatigue interaction, and creep crack growth modeling approaches used in the EPRI software programs Remaining Life Simulations and Monitoring (RLSM) and Boiler Life Evaluation and Simulation Software (BLESS) and to compare them with API 579-1/ASME FFS-1, 2007 Edition. *Creep damage* is generally defined as a reduction of a component's ability to resist stress at elevated temperature. The rate of creep damage accumulation increases with temperature and is a significant contributor to boiler tube damage and failure because the tubes typically operate in the creep temperature range (≈1000ºF [538ºC]) for the materials in use.

The specific sections of API 579-1/ASME FFS-1, 2007 Edition, that cover the damage assessments performed as part of this study are:

- 10.5.2 Creep Rupture Life
- 10.5.3 Creep Fatigue Interaction
- 10.5.4 Creep Crack Growth

In addition, the applicable sections of Annexes B.1, D, and F are used as necessary to perform the damage assessments.

The software packages RLSM and BLESS were developed for EPRI by Structural Integrity Associates (SIA). Neither program incorporates the MPC Omega model. BLESS is the most recently updated program, and it performs only crack growth rate studies. For the purposes of the current study, the API 579-1/ASME FFS-1, 2007 Edition, creep-fatigue interaction was compared with RLSM, while the Standard's creep-fatigue crack growth methodology was compared with BLESS.

The RLSM program has the capability to model both creep-fatigue interaction and creep-fatigue crack growth [3]. Both models rely on what RLSM calls "transfer" functions, which take plant readings of temperature and pressure and convert them to stress values. RLSM has the ability to relate both pressure and temperature to axial and hoop stresses, in addition to having a specified deadweight stress. It has separate transfer functions for what it calls "fatigue stress" and "creep stress." The intention behind the different categories is that the creep stress represents the relaxed stress state of the components for an in-service power plant. This is the stress used for the creep damage calculation. SIA indicated that an updated version of the program calculates stress relaxation in real-time [2], which would be required to accurately model the stress states for a new power plant. The fatigue stress represents the cyclic stress used for fatigue calculations.

The examples prepared considered 2¼ Cr – 1 Mo and 9 Cr – 1 Mo at "creep stresses" below the ASME Section II Code allowable stress for the temperature range of 900°F to 1100°F. The study consisted of the following parts:

- The LMP model for predicting time to rupture, as implemented in API 579-1/ASME FFS-1, 2007 Edition, and the RLSM software, was compared with the MPC Omega method time to rupture correlation—from API 579-1/ASME FFS-1, 2007 Edition.
- Fatigue life data sources are presented.
- The creep-fatigue interaction method of RLSM has been discussed and compared with the approach of API 579-1/ASME FFS-1, 2007 Edition.
- Comparison of the creep range crack growth method in the BLESS program versus the corresponding method in API 579/ASME FFS-1, 2007 Edition.

For brevity, the reader should take note that API 579-1/ASME FFS-1, 2007 Edition, will be referred to as "Standard' or API 579/ASME FFS for the remainder of this report.

Conversion Factors

Conversion factors for units used in this technical update are as follows:

Type	English to Standard International Units
Force	1 ksi = 4.48 kN
Length	1 in. = 25.4 mm
Pressure	1 psi = 6.89 kPa
Temperature	°C = (°F-32) x 5/9

3
OVERVIEW OF THE OMEGA MODEL

The Omega Model was developed in the 1990s by the MPC Project Omega Program. The preceding approach (in API-579, 2000 Edition) for evaluating creep rupture life was the Larson Miller Parameter (LMP) model. The LMP model is based on the concept of activation energy, and it has been reported [5] that it predicts very long rupture lives as temperatures approach the low end of the creep regime. For the cases considered during this study, this phenomenon was not seen. It has also been reported [5] that the LMP method can often be overly conservative, while the Larson-Miller constant (C_{LMP})—usually set to 20—can occasionally introduce a nonconservative result.

Omega models the entire creep process as tertiary. It starts with a general continuum damage approach and has simple, yet rigorous, mathematical relations for computing damage and strain. The Omega curve fits were intended to describe behavior at ASME Code design allowable stresses. Literature sources that discuss the development of the Omega method [6] state that modeling only tertiary creep for in-service components is reasonable. The Omega model is reportedly simpler to implement than other approaches that model tertiary creep [6].

The Omega model expresses creep rate acceleration as a function of increasing stress, increasing damage, and microstructural changes not associated with damage in the following expression:

$$\dot{\varepsilon}_c = \dot{\varepsilon}_{co} e^{m\varepsilon_c} \times \frac{1}{e^{-p\varepsilon_c}} \times \frac{1}{e^{-c\varepsilon_c}} = \dot{\varepsilon}_{co} e^{(m+p+c)\varepsilon_c}\, \dot{\varepsilon}_c$$

This equation serves well as a creep model since creep curves tend to have exponentially shaped "tertiary" sections. The three correlating variables are:

m = Norton's exponent to account for stress increase

p = Microstructural damage exponent

c = Exponent accounting for other factors associated with the stress change

For the case where (m+p+c) ϵc > 2, then Ωp = m + p + c. Thus, the strain rate is expressed as a function of only Omega and initial strain rate. Therefore, the Omega term acts as a creep damage modulus:

$$\dot{\varepsilon}_c = \dot{\varepsilon}_{co} e^{\Omega\varepsilon_c}$$

Where $\dot{\varepsilon}_c$ is the instantaneous true strain rate at true strain εc. The Omega model has been found to work well [5] for a wide range of materials and many practical pressure vessel and piping component situations.

While creep strain rate continuously accelerates in the Omega model, the rate of damage accumulation over time, while at constant stress, is assumed to be linear. That is, the first hour and thousandth hour each have the same amount of damage accumulation. As such, linear damage calculations can be performed with Omega, as are done with LMP. The equation for time to rupture (T_{ri}), which is the expression used in the current study for computing remaining life, is as follows:

$$T_{ri} = \frac{1}{\dot{\varepsilon}_{co}\Omega_m} \qquad \textbf{Eq. 3-1}$$

The remaining expressions used in calculating initial strain rate ($\dot{\varepsilon}_{co}$) and Omega (Ω_m) are included in the Standard, Appendix B.1. The Omega and LMP material data are both based on correlations with rupture test data. With respect to RLSM, if LMP curves were generated that predicted the same rupture times as Omega, the results of the evaluation would be identical.

4
MATERIAL DATA

Creep Time to Rupture Data Sources

The Larson Miller Parameter (LMP) is the legacy approach to predicting time to rupture in API 579/ASME FFS. The LMP model offers both minimum and average time to rupture correlations, and the correlations for a number of materials are listed in the Standard's Table F.31. The equations associated with using LMP to estimate time to rupture are included in Appendix B.2. These are based on the material data provided in API 530.

In the Standard's Table F.30 [1], the Omega model includes different sets of coefficients for the same base material, depending on parameters such as heat treatment. For example, for 2¼ Cr–1 Mo, sets of Omega coefficients are available for annealed, quenched and tempered (Q&T), normalized and tempered (N&T), and 2¼ Cr–1 Mo-V. A significant number of temperature and stress range restrictions are applied to the use of many of the correlated expressions.

The Omega approach is more sophisticated in that it includes adjustment factors for creep ductility (the allowed range is +0.3 for brittle behavior and −0.3 for ductile behavior) and an adjustment factor for creep strain rate to account for the material scatter band (the allowed range is −0.5 for the bottom of the scatter band to +0.5 for the top of the scatter band). However, there is no guidance on how to determine what adjustments to apply. A description of the creep rupture life predictions is shown in Table 4-1, and the Omega equations are included in the Standard's Appendix B.1 [1].

API 579/ASME FFS LMP time to rupture comparisons were made with the Omega model for 2¼ Cr–1 Mo and 9 Cr–1 Mo in the temperature range of 900ºF–1100ºF. The stress was varied, from 0.25 ksi up to the allowable stress specified in Table A-2 of B31.1 [4], at the given temperature for each material. The results are plotted in Figures 4-1 through 4-6. Note that the RLSM comparisons made in Figures 4-1 through 4-3 use the LMP expression provided by the RLSM software in an example problem materials database; the LMP correlation coefficients can be modified by the user.

The Omega model curves published in API 579/ASME FFS have a notably different shape and diverge from the LMP prediction at low stress values, but they give similar results and curve shapes in the mid stress range. The low stress divergence is not particularly relevant since that corresponds to regions where creep rupture is not a concern. At high stress values for 2¼ Cr – 1 Mo, the models behave similarly, but there is a tendency for the LMP method to predict a longer life as the allowable stress is approached for 9 Cr – 1 Mo. There has been a great deal of work done on this alloy in recent years, so it is important that both models incorporate the latest experimental and experience-based results.

The Omega data for 9 Cr – 1 Mo at 900°F, as shown by the curve in Figure 4-4, show a large divergence from the LMP prediction. Note that the primary authors of the Omega method have indicated that this is an uncommon temperature and stress combination for this metal [14]. Since one of the considerations in setting the allowable stress is 2/3 the average stress to rupture in 100,000 hours, the stress value of the average rupture curves at 100,000 hours can be no less than 1.5 times the allowable stress. Based on this, it is not recommended that the Omega curve be used for time to rupture calculations for 9 Cr – 1 Mo at 900°F and 1000°F. It also is an indication that the material data provided in API 579/ASME FFS for the Omega model require further review for anomalies. Explicit restrictions on the applicable ranges of stress and temperature should be provided as necessary to avoid extrapolations into regimes not supported by the available data.

The RLSM LMP correlation in the example provided appears to be based on average time to rupture.

Figure 4-7 plots a comparison of time to rupture values for Omega versus LMP as a function of pressure. In contrast with Figures 4-1 through Figure 4-6 which compared rupture life results with an assumed unidirectional stress, the calculations in Figure 4-7 were obtained by varying the pressure and calculating the resulting hoop, axial, radial, and Von-Mises stresses, using both thin-walled and non-thin-walled assumptions. These stresses were input into the time to rupture correlations. For this case, where multi-directional stresses were considered and plotted as a function of the operating pressure, it can be seen that the Omega and LMP predictions are closer than the unidirectional stress case considered in Figure 4-3.

Table 4-1
Creep Time to Rupture Correlation Comparisons

Model	Comments
API 579/ASME FFS Larson Miller Parameter (Equations in Appendix B.2)	Table F.31 contains coefficients for both minimum and average time to rupture. Coefficients are not heat-treatment-dependent or temperature limited. Controlling stresses are principal and Von-Mises.
API 579/ASME FFS MPC Project Omega (Equations in Appendix B.1)	Restrictive temperature and stress limitations. Coefficients are dependent on heat treatment. Coefficients are center of scatter band from service-aged materials at design stress levels. Controlling stresses are principal and Von-Mises. This material model allows for adjustment due to ductility and position on the scatter band, but no guidance is given on how to apply these adjustments.
RLSM	RLSM uses its materials database, which includes user input coefficients for the LMP curve (3rd order polynomial function of $\log_{10}$(stress)). The RLSM materials database allows modifications of the coefficients, so any dataset presumably can be fit to this curve, and the time to rupture results in theory can replicate those of the API 579/ASME FFS LMP approach if the curve fit is accurate.

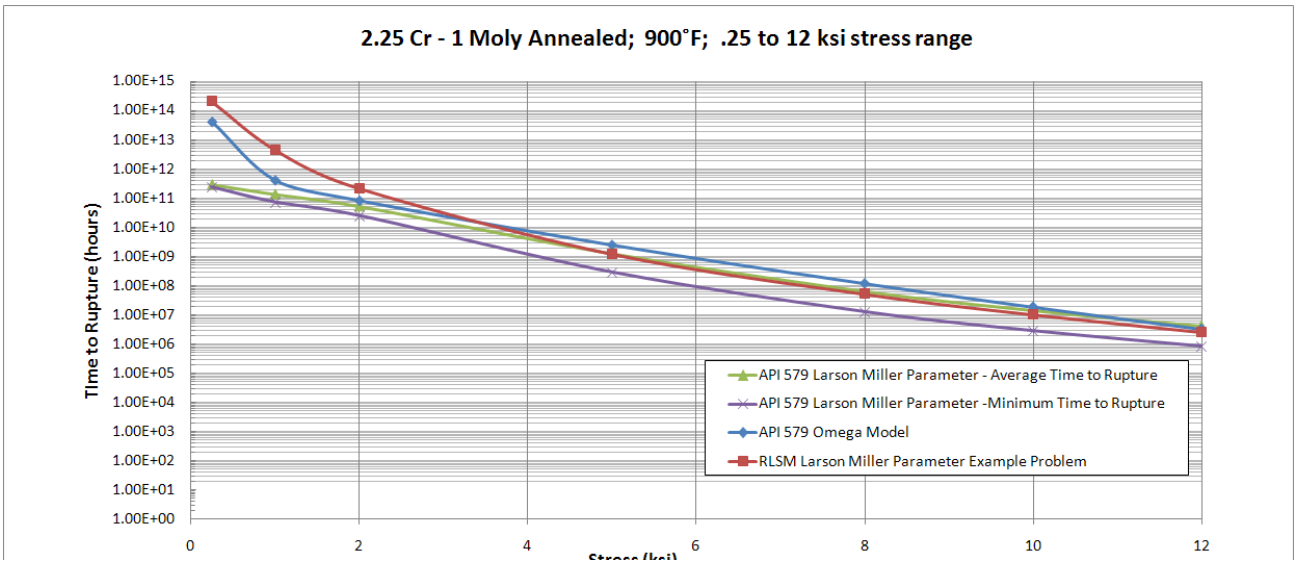

Figure 4-1
Time to Rupture Comparison: 2¼ Cr – 1 Mo Annealed, 900ºF, 0.25–12 ksi Stress Range

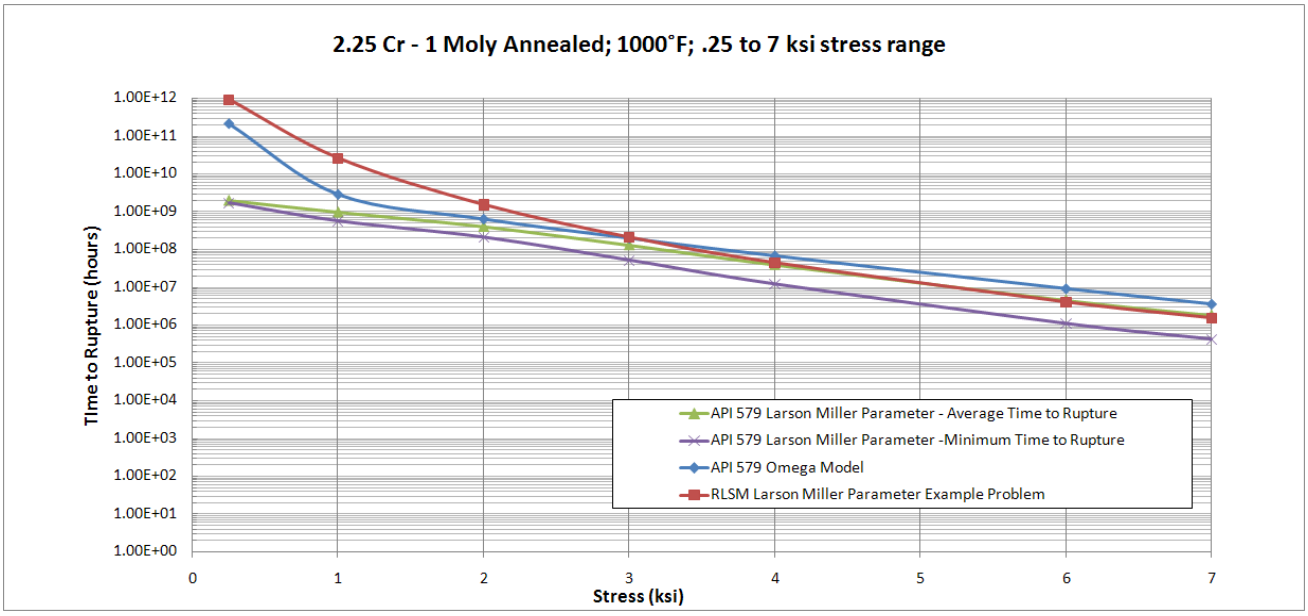

Figure 4-2
Time to Rupture Comparison: 2¼ Cr – 1 Mo Annealed, 1000ºF, 0.25–7 ksi Stress Range

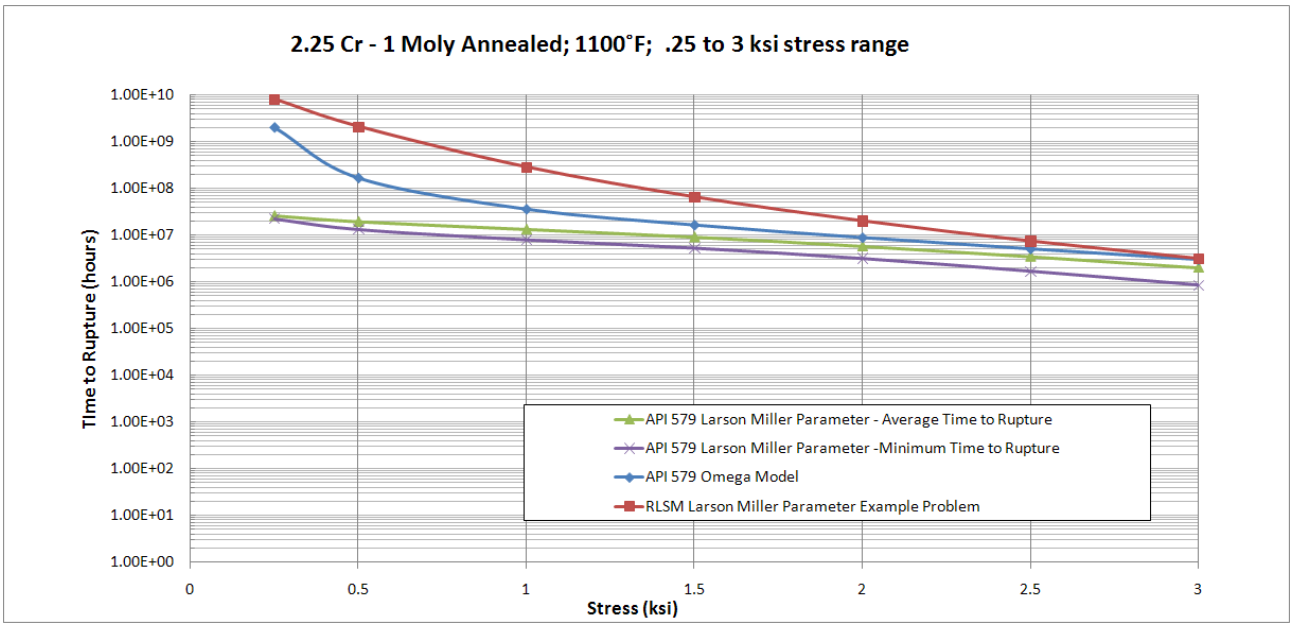

Figure 4-3
Time to Rupture Comparison: 2¼ Cr – 1 Mo Annealed, 1100ºF, 0.25–3 ksi Stress Range

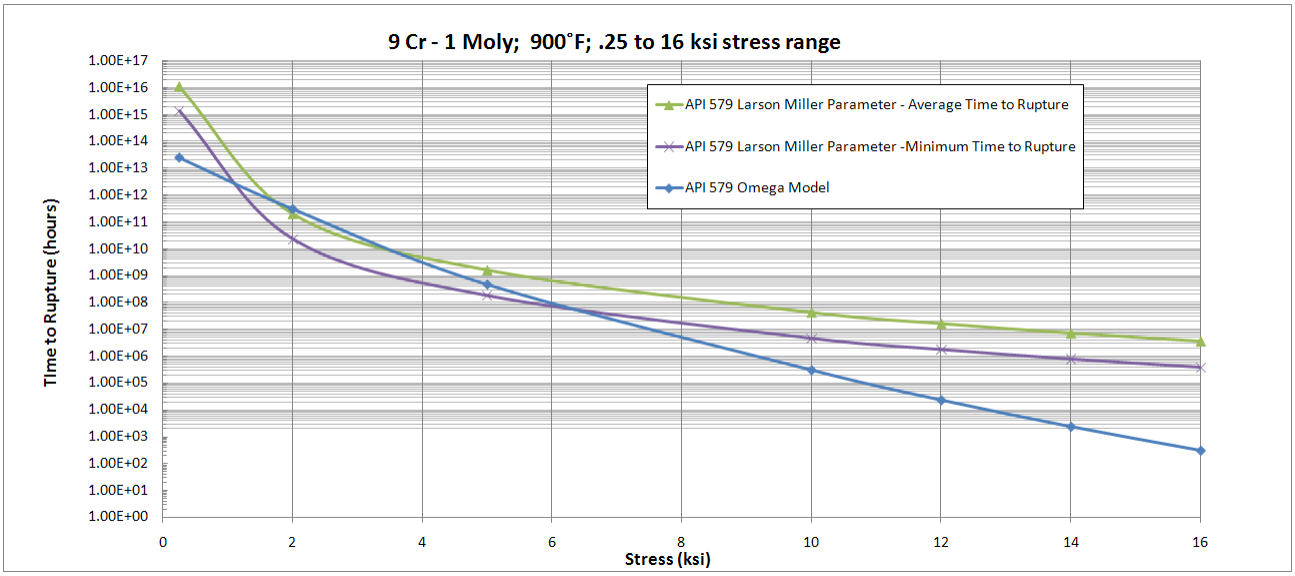

Figure 4-4
Time to Rupture Comparison: 9 Cr – 1 Mo Annealed, 900ºF, 0.25–16 ksi Stress Range

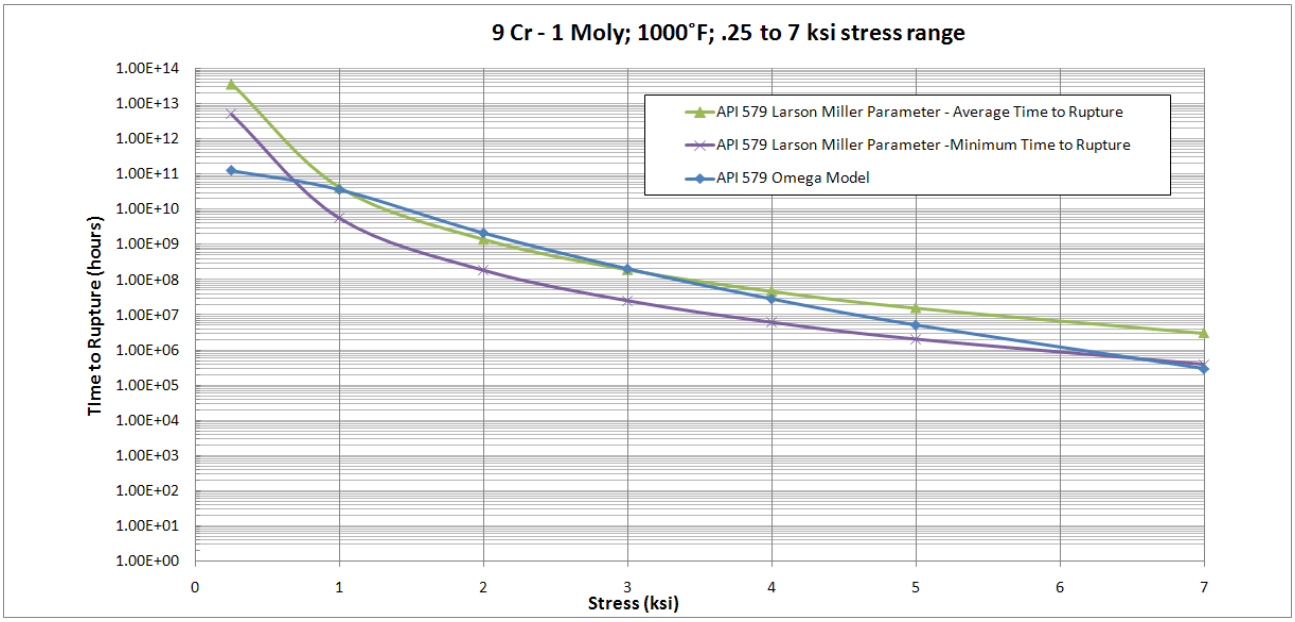

Figure 4-5
Time to Rupture Comparison: 9 Cr – 1 Mo Annealed, 1000ºF, 0.25–7 ksi Stress Range

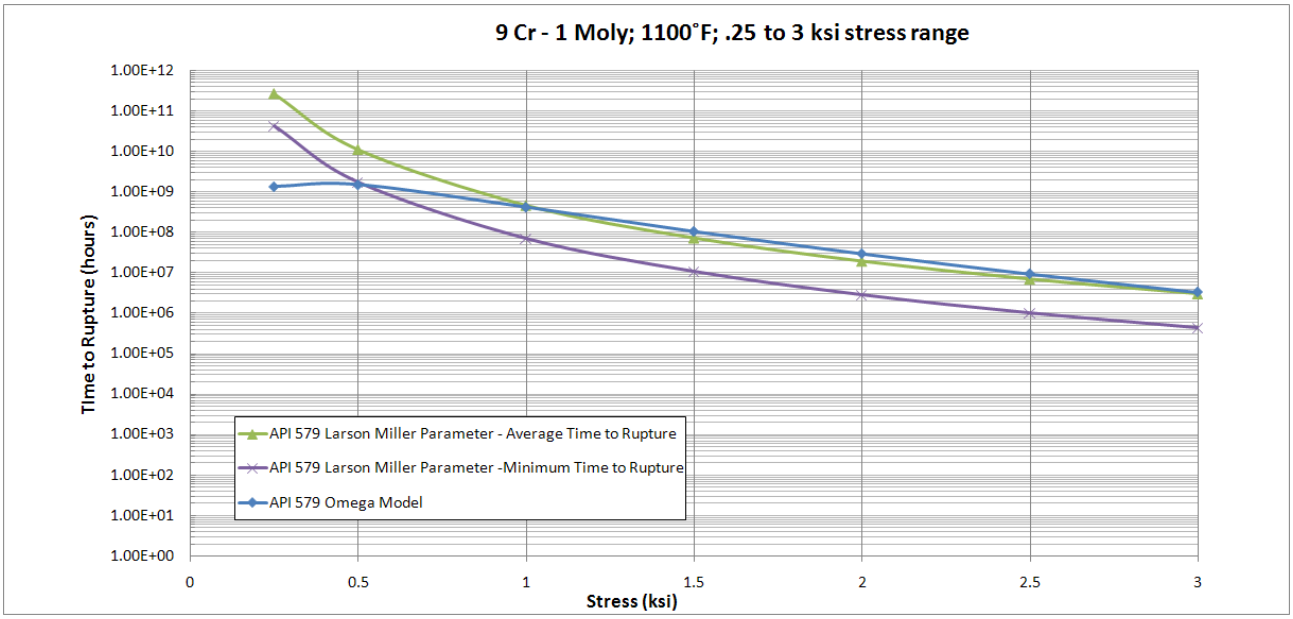

Figure 4-6
Time to Rupture Comparison: 9 Cr – 1 Mo Annealed, 1100ºF, 0.25–3 ksi Stress Range

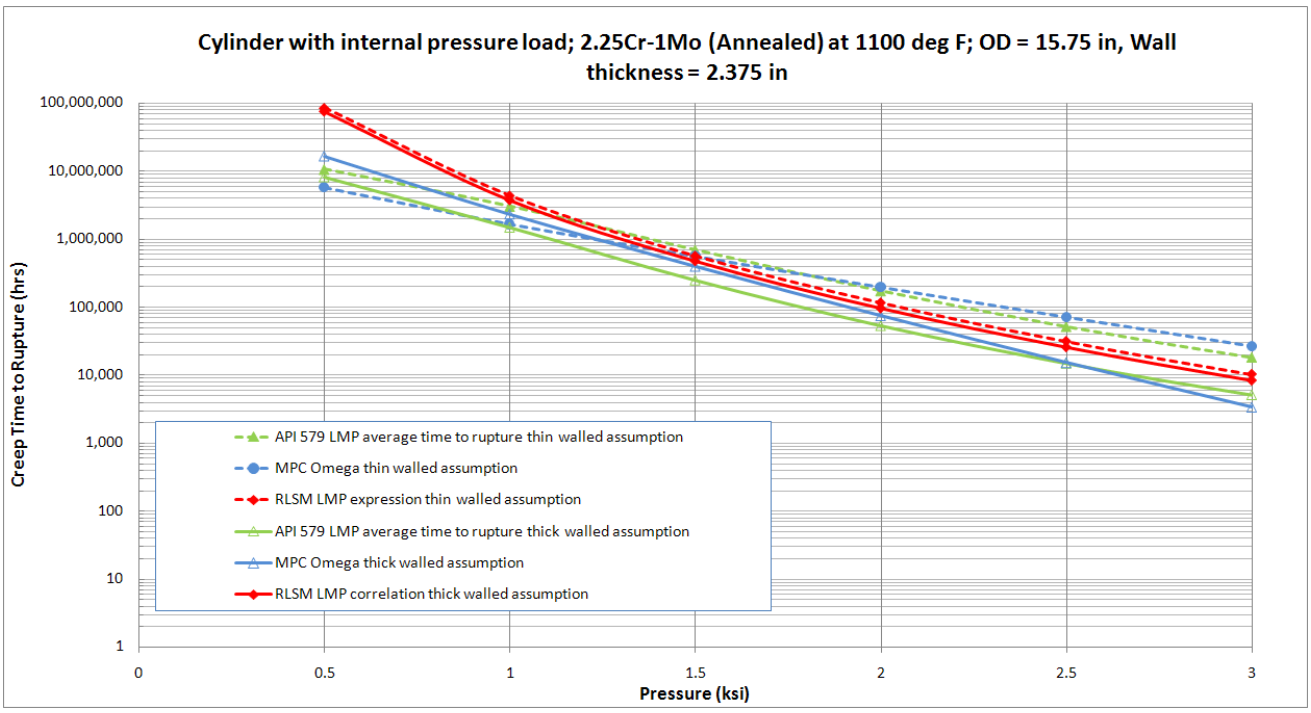

Figure 4-7
Time to Rupture Comparison Correlated with Internal Pressure Only Load

Table 4-2 documents a comparison of time to rupture calculations for a fixed uniaxial stress state that was chosen not to exceed the allowable stress for all temperatures and materials considered. The temperature range for this comparison is 900ºF to 1100ºF. The average LMP model predicts lower average rupture lives for 9 Cr – 1 Mo and 2¼ Cr – 1 Mo compared with Omega at this low stress value.

Table 4-2
Comparison of API 579-1/ASME FFS-1 Correlations for Time to Rupture at 2.8 ksi (5) Using Omega, Larson Miller Parameter (LMP) Average, and LMP Minimum Material Models

2¼ Cr – 1 Mo	Tr @ 1100 ˚F (hrs)	Tr @ 1000 ˚F (hrs)	Tr @900 ˚F (hrs)
MPC Project Omega (1), (2), (3)	3,659,345	241,824,010	29,597,615,785
LMP - Average time to rupture (4)	2,551,773	164,259,272	19,507,481,771
LMP -Minimum time to rupture (4)	1,118,940	68,072,520	7,577,289,410
9 Cr – 1 Mo			
MPC Project Omega (1), (2)	4,939,679	319,823,921	38,236,481,750
LMP - Average time to rupture (4)	4,079,584	271,181,965	33,415,021,454
LMP -Minimum time to rupture (4)	605,432	35,315,109	3,745,811,212

Notes:

(1) Coefficients in this table are estimates of the typical material behavior (the center of the scatter band) based on the MPC Project Omega materials data from service-aged materials at design stress levels.

(2) The Omega data are intended to describe material behavior in the range of the ASME Code design allowable stress for a given material at a specified temperature.

(3) 2¼ Cr – 1 Mo (Annealed) and 9 Cr – 1 Mo have been used. The Omega method provides different sets of coefficients for different heat treatment conditions for the 2¼ Cr – 1 Mo material. Some regions of large discrepancies between Omega and LMP were found for the conditions studied. These curves can be expected to provide good agreement only in the case where they are near to actual operating conditions used to produce the curves. For example, according to the primary authors of the Omega model, predictions of 9 Cr –1 Mo at 900°F are based on extrapolation of existing data [14]. This is not a common operating condition for this metal; therefore, existing rupture data do not include this case.

(4) The fact that the Standard does not specify valid use ranges for the Omega material model represents a potential pitfall for the novice user of API 579/ASME FFS. This is an important future enhancement for API 579/ASME FFS.

(5) Data for the minimum and average LMPs in this table are from Figures 4-A through 4-S of API STD 530 [17], "Calculation of Heater Tube Thickness in Petroleum Refineries."

(6) Stress = 2.8 ksi was selected to not exceed the minimum allowable stress value for all conditions considered.

Observations on Creep Rupture

1. Determining an appropriate creep stress has a very substantial effect on the creep damage calculation. If the initial stress rather than a relaxed stress is input, the calculation of damage will be very conservative.
2. It appears from comparison of the RLSM example problem and API 579/ASME FFS LMP data in Figures 4-1 through 4-3, that the RLSM creep rupture model in the example problem is based on average properties. Note that this is a user input; alternatively, minimum time to rupture data can also be used.
3. Using an effective stress rather than a maximum principal stress can create significant differences in life prediction; however, B31.1 piping stress analysis does not provide information from which the effective stress can generally be determined in particular in components such as elbows and tees, which often are the governing locations in a piping system.
4. The damage calculation procedure is the same in RLSM as in API 579-1/ASME FFS-1: linear time fraction damage. As such, if the stress and material rupture properties are the same, the calculated damage per unit of time will be the same.
5. Even if the same creep rupture material data are used with RLSM and API 579-1/ASME FFS-1, the life predictions can be different because of how the stresses are evaluated. The effective stress per API 579-1/ASME FFS-1 can be higher or lower than the maximum principal stress. For example, a 2:1 biaxial tension stress state, which is that of a pressurized cylinder, has an effective stress that is less than the maximum principal stress. It is less damaging than a uniaxial tension case with a stress value equal to the maximum principal stress of the biaxial case. Note, however, that effective stresses are not an available output from B31.1 piping stress analysis results except at locations with very simple geometries, such as cylinders. Information on the three-dimensional stress state at, for example, a tee, is not readily available. As such, application of these rules for typical piping is not practical.

Fatigue Life Data Sources

There are two distinct methods of evaluating fatigue life in the Pressure Vessel Codes and Piping Codes [7]. The first is based on actual component test data and the other is based on smooth bar testing. A fatigue analysis based on smooth bar testing requires additional factors to account for stress concentrations.

The original source of component test data for the B31 piping codes and subsections NC and ND in ASME Section III come from tests performed by Markl [7]. These tests were performed using butt welded pipe. Industry practice typically applies a factor of two on the stress calculated by a typical stress analysis program (for example, a B31.1 piping flexibility analysis program) to account for the stress intensification due to the weld when comparing the results to smooth bar fatigue curves [7]. The stress calculated using these programs, following code rules, is intended to be compared to welded pipe fatigue curves, not smooth bar fatigue curves. The factor of two considers the difference between these two fatigue curves.

The RLSM fatigue analysis appears to be based on subsection NB of Section III, which is the sole ASME piping code that uses smooth bar fatigue curves. This approach requires the user to

determine the alternating stress intensity per NB-3216.1(c) [8]. This is inconsistent with the information in the RLSM manual, which indicates that the stress information for the transfer functions should come from the B31.1 stress reports. Using the B31.1 stress report results would result in using about one-half the value of stress that should be used when applying it to a smooth bar fatigue curve.

In the Section VIII Division 2, 2007 Edition, the required stress is the alternating Von Mises stress. RLSM uses the maximum principal stress of either the hoop or axial direction for fatigue evaluation. It does not appear to include compressive radial stresses that occur at the bore due to internal pressure, which means there are situations where using the maximum principal stress could result in a nonconservative estimate of stress. Additionally, if there were longitudinal compression combined with hoop tension, the use of a maximum principal stress to evaluate fatigue life would be nonconservative. The user of RLSM could artificially bypass this problem by defining the hoop or axial stress as equivalent to the stress intensity; however, this would not be an intuitive step. Additionally, it is important that users be aware of the stress states that are entered into RLSM because some plants' piping reports conform to B31.1, as noted in the RLSM documentation [3]. Stresses from such an analysis must be multiplied by a factor of about 2 when compared to a smooth bar fatigue curve. Section VIII Division 2 lists appropriate stress intensification factors for different potential stress concentrators, whereas subsection NB of Section III leaves it to the engineer's judgment.

API 579/ASME FFS refers the user to Tables in Appendix F [1] for fatigue data. The lower temperature (700ºF) correlations tabulate fatigue life with stress amplitude, defined as one-half the effective total equivalent stress range, while for the creep temperature range, the independent variable used to predict fatigue life is the strain range. The lower temperature fatigue curves are from the ASME B&PV Code, Section VIII, Division 2. The creep range, or high-temperature, curve fits in the Standard are derived from tabular data from the ASME Boiler and Pressure Vessel Code Section III, Subsection NH [9]. Figure 4-8 shows plots of the published high-temperature fatigue curves for 2¼ Cr – 1 Mo and 9 Cr – 1 Mo as a function of strain range.

Currently, there are proposed updates to the Standard's creep range curve fits to both the ASME Boiler and Pressure Vessel, Section VIII, Division 2 and the Section III, Subsection NH data. The current study has used these new proposed coefficients for the comparisons made in the current study because they represent improved fits to the data.

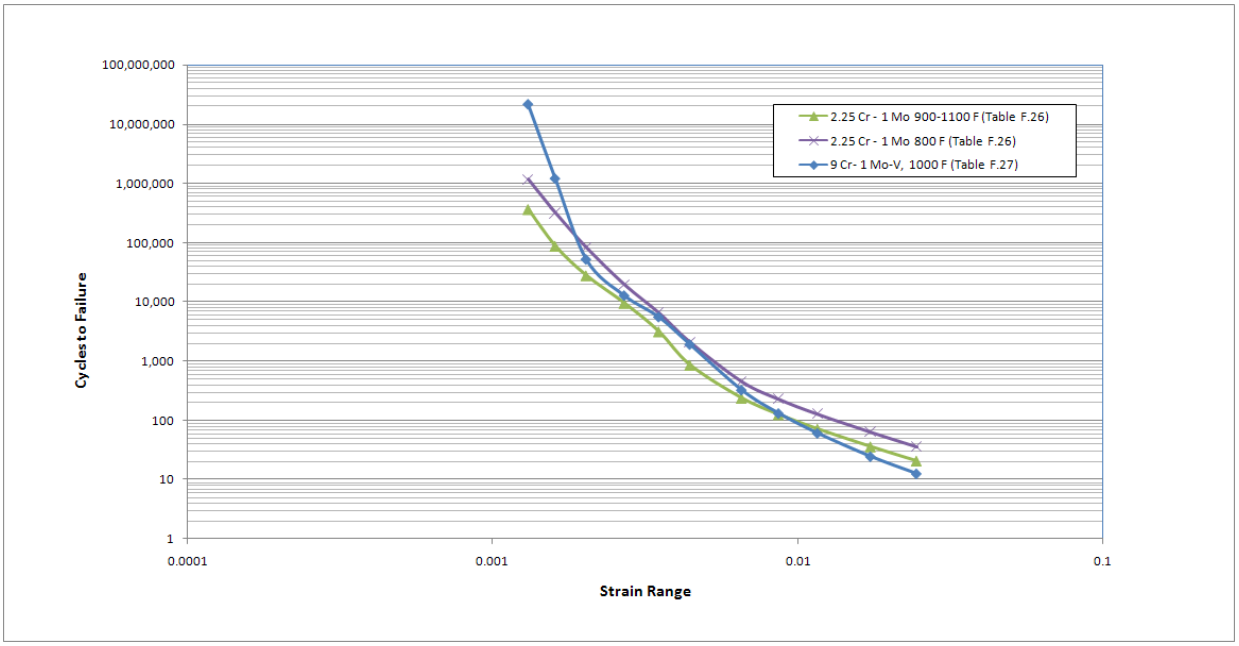

Figure 4-8
API 579-1/ASME FFS-1, 2007 Edition Fatigue Curves (proposed)

5
CREEP TIME TO RUPTURE MODELING

RLSM Creep Time to Rupture Methodology

RLSM uses an LMP formulation for calculating the accumulation of creep damage. Based on benchmarking shown in Appendix A, the project team determined that RLSM uses the largest principal stress from the creep stress correlations for axial and hoop stress. The LMP formulation is based on the following curve fit:

$$LMP = c_0 + c_1 \log\sigma + c_2(\log\sigma)^2 \quad \textbf{Eq. 5-1}$$

$$\log_{10} T_{ri} = \frac{LMP}{T+460} - 20 \quad \textbf{Eq. 5-2}$$

Where:

σ is the maximum principal stress.
T is temperature in degrees F.
T_{ri} is time to rupture for the current operating period t_i.

Creep damage is then accumulated over time using a time fraction rule:

$$D_c^m = \sum_{i=1}^{m} \frac{t_i}{T_{ri}} \quad \textbf{Eq. 5-3}$$

Total accumulated creep damage ($D_c = \sum_{m=1}^{M} D_c^m$) over all load cycles is compared to the total allowable creep damage specified in the location definition database.

API 579/ASME FFS Creep Time to Rupture Methodology

This assessment is applicable to components that are operating in the creep range with a steady-state loading condition and do not have crack-like flaws. The Level 2 assessment procedure per API 579/ASME FFS involves evaluating the temperature profile, load component, and stress components for the current time period (t_i). These are the inputs to the LMP or Omega model for determining time to rupture for the current time period (T_{ri}) as discussed in Section 4. As in RLSM, the creep damage for each time increment is accumulated for the m_{th} cycle of operation using the time fraction rule (see Equation 5-3).

For the Omega model, Equation 5-3 can be further developed as follows:

$$D_c^m = \sum_{i=1}^{m} \frac{t_i}{T_{ri}\{\Omega\varepsilon_c\}} = \sum_{i=1}^{m} \frac{t_i}{1/(\Omega\dot{\varepsilon}_c)}$$

Eq. 5-4

This procedure is repeated for all operation cycles. The standard recommends that the sum of the creep damage for all operation cycles should not exceed 0.8 or the following unless there is good justification for an alternative value:

$$D_c = \sum_{m=1}^{M} D_c^m \leq 0.8$$

Eq. 5-5

As previously discussed, the API 579/ASME FFS creep rupture method allows for use of either the LMP or Omega models, with Omega being the preferred approach. Another important distinction is that the material data from the Omega model can be used directly to model creep behavior in an inelastic finite element analysis by implementing the following relationship for the creep strain rate:

$$\dot{\varepsilon}_c = \dot{\varepsilon}_{co} e^{\Omega\varepsilon_c}$$

Eq. 5-6

Figures 5-1 and 5-2 show the difference in rupture time estimates by simulating Equation 5-3 until $D_c = 1$ using average LMP (Equation 5-3) and Omega (Equation 5-4) for two examples.

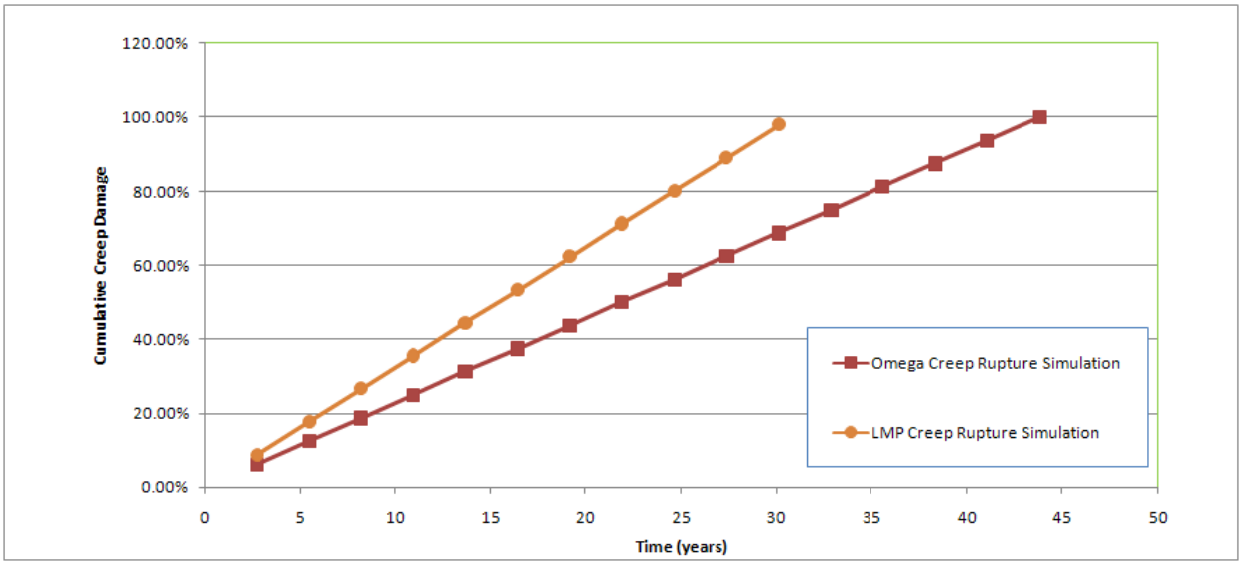

Figure 5-1
Comparison of Differences in Creep Rupture Simulations Using LMP Average and Omega Models: Unidirectional Stress = 9.5 ksi, 2¼ Cr – 1 Mo (Annealed), 1000ºF

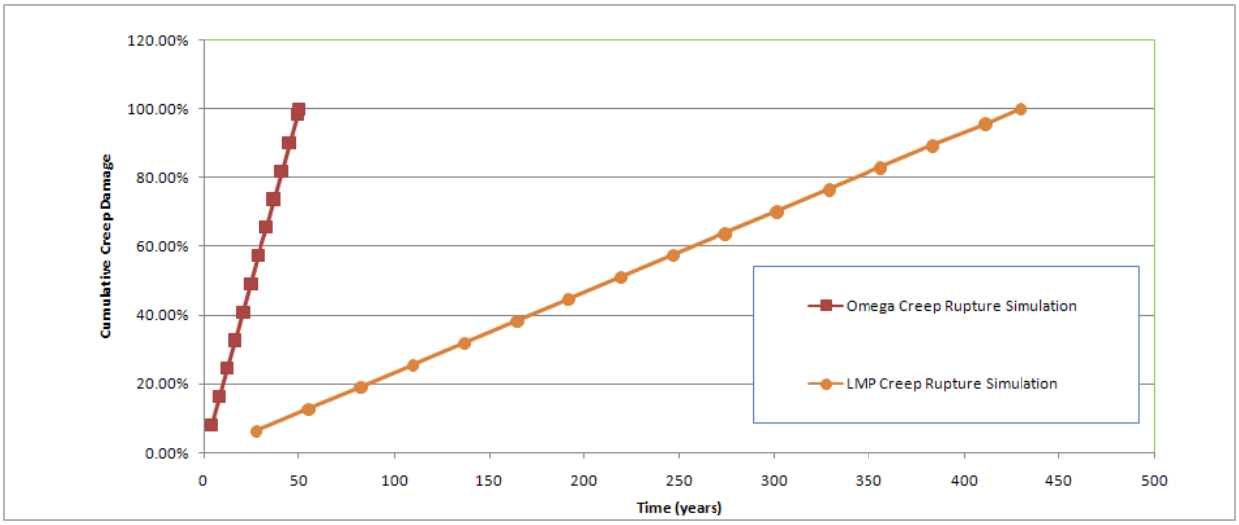

Figure 5-2
Comparison of Differences in Creep Rupture Simulations Using LMP Average and Omega Models: Omega Unidirectional Stress = 6.7 ksi, 9 Cr – 1 Mo (Annealed), 1000ºF

Table 5-1 tabulates rupture time in years for a number of cases, including those plotted in Figures 5-1 and 5-2. For LMP, the average life is presented in order to be consistent with Omega. These results, along with the time to rupture plots of Figures 4-1 through 4-6, show that substantially different results can be obtained with the available data in API 579/ASME FFS. As previously noted, the material data used for Omega for 9 Cr – 1 Mo appears to be in error at 900°F and questionable at 1000°F.

Both the rupture life predictions using LMP and Omega are simply based on curve fits of the available creep rupture data. No conclusions can be drawn as to which is a better representation of the actual rupture life, but some situations have been seen where Omega results should be further reviewed.

Table 5-1
Rupture Time in Years Comparisons

Material	Temperature (F)	Stress (ksi)	LMP Avg Rupture Life (yrs)	Omega Rupture Time (yrs)
2¼ Cr – 1 Mo	900	14.5	130	48
2¼ Cr – 1 Mo	1000	9.5	30.1	44
9 Cr – 1 Mo	900	9.7	5500	52
9 Cr – 1 Mo	1000	6.7	429	50

Observations on Creep Rupture Methodologies

1. RLSM uses an LMP approach that is a simple polynomial fit to the maximum stress for predicting creep time to rupture. In practice, this approach can be used to return essentially the same results as the Average LMP, Minimum LMP, or Omega correlations that are in API 579/ASME FFS. As a result, a curve fitting exercise is required to duplicate the Standard's

material model data. The Omega data fitting exercise is potentially complicated for use in RLSM if a number of operating conditions are to be simulated.

2. RLSM does not have the ability to model creep damage as a function of a multi-dimensional stress state.
3. Both RLSM and API 579/ASME FFS accumulate creep damage using a time fraction approach.
4. RLSM uses principal stress, whereas API 579/ASME FFS uses effective stress. However, the transfer functions in RLSM could be used to calculate effective stress, if it were known. Note that effective stress is not generally available from pipe stress analysis results.

6
FATIGUE DAMAGE METHODOLOGY

RLSM Fatigue Methodology

The RLSM fatigue analysis is based on a smooth bar fatigue curve as described in Section 4.2. RLSM has fatigue stress correlations for temperature and pressure that presume independence from the creep stress correlations. The correlations include an axial dead weight stress and expansion/pressure stresses for both the axial and hoop directions. In addition to these stress correlations, RLSM considers the effect of thermal stresses due to temperature gradients through the pipe wall thickness in the calculation of the total stress range [10].

RLSM does not perform any stress calculations except for a thermal stress calculation using the Green's function for the through wall temperature gradient. The RLSM documentation mentions ASME B31.1 stress reports as a potential source for stress values [4]. Additionally, in email correspondence with SIA [10], it was noted that they also refer to Subsection NB of ASME Section III for the fatigue analysis, and this is consistent with the use of the smooth bar fatigue curves. It is very important that any users of RLSM recognize the large difference in stresses calculated in accordance with ASME B31.1 and Subsection NB of ASME Section III. The stress calculated by Equation 11 in Paragraph NB-3653.2(a) of Subsection NB is approximately two times the stress calculated by Equation 13A in Paragraph 104.8.3 of B31.1. Therefore, any stresses calculated by B31.1 cannot be compared to smooth bar fatigue curves without an appropriate adjustment, essentially a factor of two increase in longitudinal stress (not hoop stress) for fatigue calculations).

RLSM bases the fatigue stress range on the maximum principal stress just as it does for the creep stress. RLSM uses an Ordered Overall Range (OOR) method to determine each stress range [3]. The stresses are then altered by the modulus of elasticity correction in order to compare them to the smooth bar fatigue curves. This correction is performed because the smooth bar fatigue curves are actually based on strain; however, they are plotted versus stress based on the modulus of elasticity of the test specimen. While any fatigue data could be entered into the database, the project team found the traditional carbon-steel low-alloy data for temperatures less than 700^{o}F in the example databases.

A simple benchmark was performed, shown in Appendix A.2, and results were close to the RLSM output. Important to this comparison is that—as explained by SIA—RLSM rounds the lower bound stress value down to the nearest integer value and the upper bound stress value up to the nearest integer value. Once this rounding method was implemented, the total difference in accumulated damage was only 8%. This is explained by the inclusion of thermal stress as detailed by SIA [10]. The additional conservatism introduced by only using integer values for determining the stress range is unnecessary because RLSM is able to report the fatigue stresses at any point in time in a decimal format.

API 579/ASME FFS Fatigue Methodology

If load cycles are present for the component, then fatigue damage is calculated to estimate fatigue remaining life. The load history is determined and divided into operating cycles. The fatigue data used by API 579/ASME FFS is described in Section 4.2 and, for the creep temperature range, correlates strain range with fatigue life (N_{fi}).

The fatigue damage is accumulated for each load cycle as follows:

$$D_f = \sum_{i=1}^{m} \frac{1}{N_{fi}} \qquad \textbf{Eq. 6-1}$$

Observations on Fatigue Methodologies

1. Both RLSM and API 579/ASME FFS use conventional cycle fraction damage calculations
2. RLSM uses principal stress, whereas API 579/ASME FFS uses effective stress. However, the transfer functions in RLSM could be used to calculate effective stress, if it were known. But effective stress is not generally available from pipe stress results.
3. RLSM uses some rounding up of the fatigue stress amplitude and, along with some other small differences, gives a slightly more conservative result. For the cases considered in this study, fatigue damage was about 8% higher in RLSM when directly compared with API 579/ASME FFS.
4. The user needs to be informed and aware so as not to use a B31.1 [4] pipe stress analysis result in conjunction with the smooth bar fatigue data in RLSM.

7
CREEP-FATIGUE INTERACTION

RLSM Creep-Fatigue Interaction Methodology

RLSM sums the monitored fatigue damage and monitored creep damage to arrive at "total current damage." This damage is compared to a user-entered allowable damage that is specified in the location description database. For example, if the allowable damage were 0.3, Figure 7-5 shows the RLSM creep-fatigue envelope that would result. The predicted life based on such an envelope would be very short compared to the creep-fatigue damage envelope from API 579/ASME FFS (as shown in Figure 7-5) unless the creep and fatigue damage accumulate at the same rate. Appendix A.3 shows an example problem that documents RLSM's creep-fatigue interaction.

API 579/ASME FFS Creep-Fatigue Interaction Methodology

This procedure is applicable to components that do not contain crack-like flaws and are operating in the creep range under cyclic loading conditions. Creep fatigue interaction is defined as a situation where a combination of the following may occur:

- Time-dependent straining and damage
- Varying stresses (loads, including startup and shutdown) leading to damage
- Creep damage and fatigue damage interacting to further shorten life

Literature sources [5] cite a strong interaction of creep and fatigue damage mechanisms. For example, the data in Figure 7-1 show that at failure:

$$D_f + D_c \neq 1 \qquad \textbf{Eq. 7-1}$$

Instead literature sources recommend the following relationship:

$$\sqrt{D_f} + \sqrt{D_c} = 1$$

Figure 7-2 shows the plot specified in API 579/ASME FFS for determining the acceptance criterion using calculated fatigue damage (D_f) and creep damage (D_c).

The procedure involves calculating D_f for each load operating cycle according to Equation 6-1. D_c, which is time dependent, is calculated from Equation 5-5 and integrated according to the selected time increments throughout the load cycle. D_f and D_c are plotted on Figure 7-2 at the end of each operating cycle.

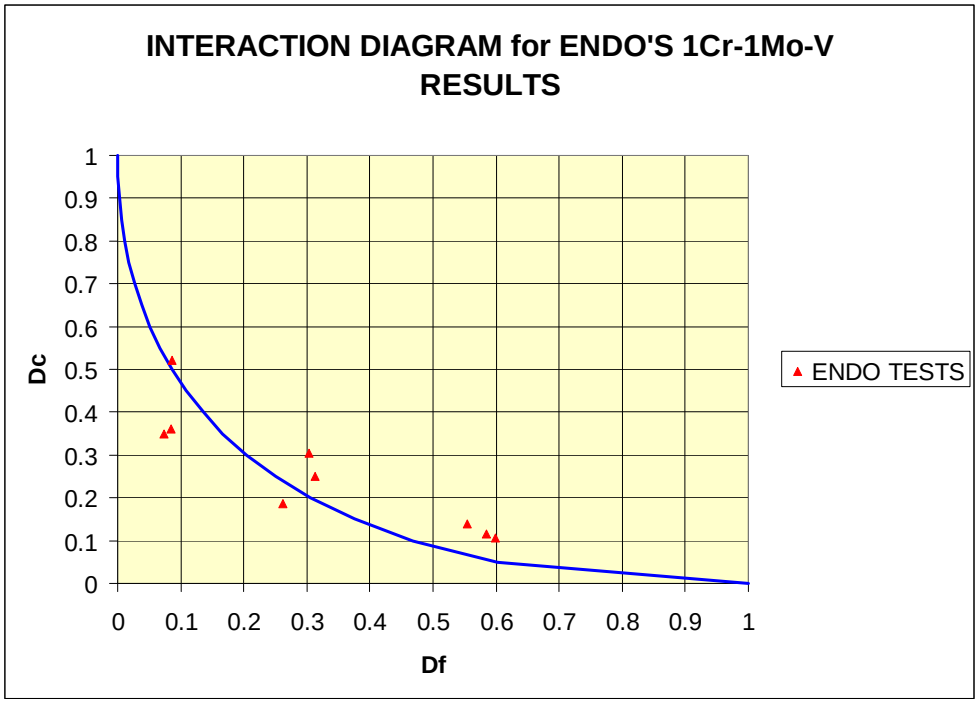

Figure 7-1
Sample Data Demonstrating Creep-Fatigue Interaction [5]

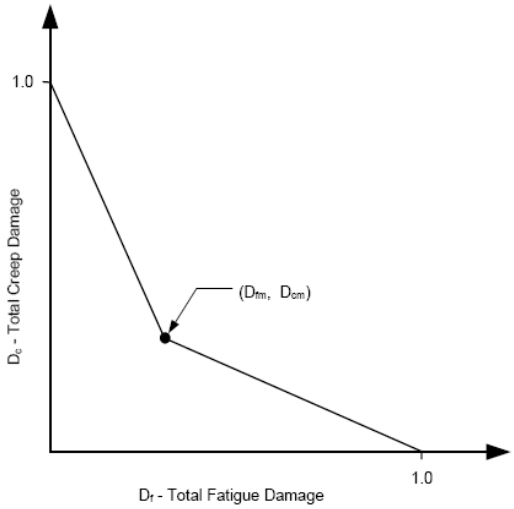

Material Parameters to Define the Acceptable Creep-Fatigue Envelope

Material	D_{fm}	D_{cm}
Carbon Steels	0.15	0.15
Low Alloy Steels	0.15	0.15
Type 304 SS	0.30	0.30
Type 316 SS	0.30	0.30
Alloy 800H	0.15	0.15

Figure 7-2
API 579/ASME FFS Creep-Fatigue Damage Acceptance Criterion

Creep-Fatigue Interaction Examples

The example shown in Figures 7-3 through 7-5 considered the case of 2¼ Cr – 1 Mo with a 300-hour load cycle and conducted the analysis according to API 579/ASME FFS using both Omega and Average LMP data. Table 7-1 describes the 300-hour operating cycle. The operating creep stress was set just below the ASME Code Allowable Stress at 2.9 ksi. This is because the creep stress is intended to be the fully relaxed stress state, which was assumed to be about equal to the allowable stress. The fatigue amplitude per cycle was set to be 21 ksi, which is the stress range. These were arbitrarily selected values to illustrate the methodology because using the same stress values for fatigue and creep would give no fatigue damage over time. Two of these cycles are shown in Figure 7-3.

Table 7-1
Cycle Description of Creep Fatigue Interaction Example: 2¼ Cr – 1 Mo

Time	Temperature (F)	Axial Stress (ksi)	Hoop Stress (ksi)
1–10 hours	70	2.8	0
>10–20 hrs (1)	70–1100	2.8–45	0–2.8
>20–290 hrs	1100	45	2.8
>290–300 hrs (1)	1100–70	45–2.8	2.8–0

(7) **Notes:**
(1) Linear ramping between conditions occurred.

(8) (2) Fatigue stress amplitude for each of the 300-hour load cycle = (45-2.8)/2 = 21.1 ksi.

(9) (3) Creep stress is maintained below ASME Code allowable (Max creep stress = 2.8 ksi).

The case was simulated using both LMP and Omega material models until failure. The creep damage was calculated and accumulated on an hourly basis, whereas the fatigue damage was calculated and accumulated at the end of each load cycle, or at each 300-hour increment. The fatigue and creep damage were plotted versus time in Figure 7-4 and also plotted on the failure envelope diagram of API 579/ASME FFS in Figure 7-5.

The fatigue damage over time is identical as expected since the fatigue curves used in each simulation are the same. The Omega method accumulates creep damage more slowly in this case because it has a longer predicted time to rupture for the creep condition considered.

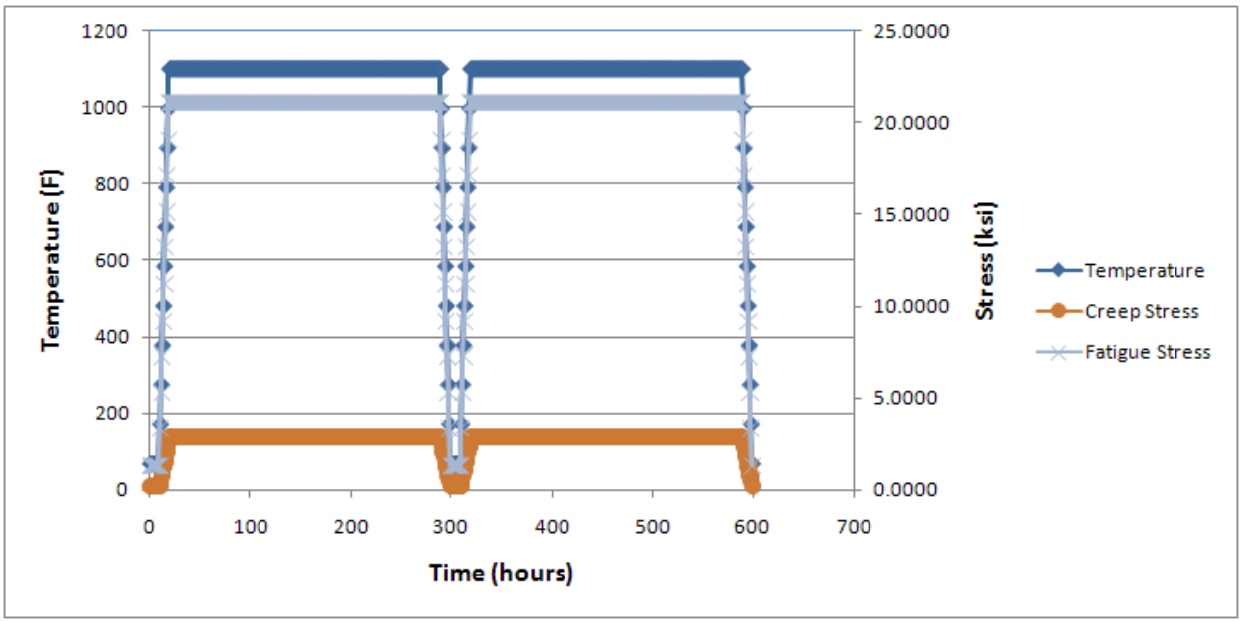

Figure 7-3
Temperature and Load Cycle for Creep-Fatigue Examples: 300-Hour Cycle; Two Cycles Are Shown

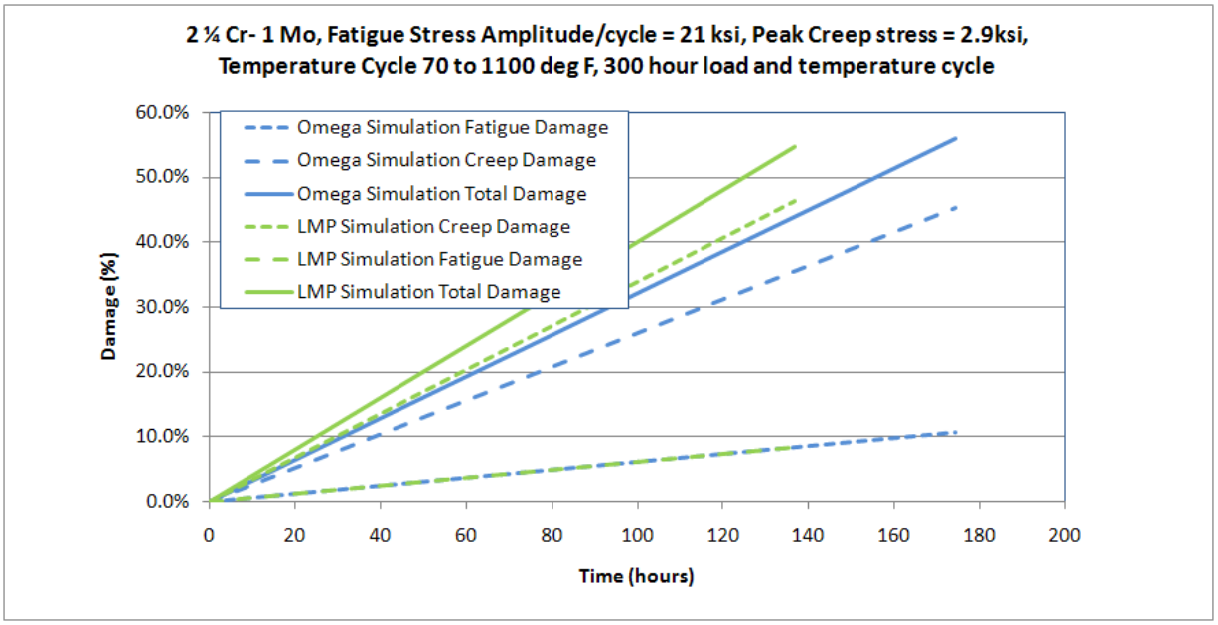

Figure 7-4
Plot of Fatigue Damage, Creep Damage, and Total Damage for Creep-Fatigue, Example 1: Omega versus LMP Method

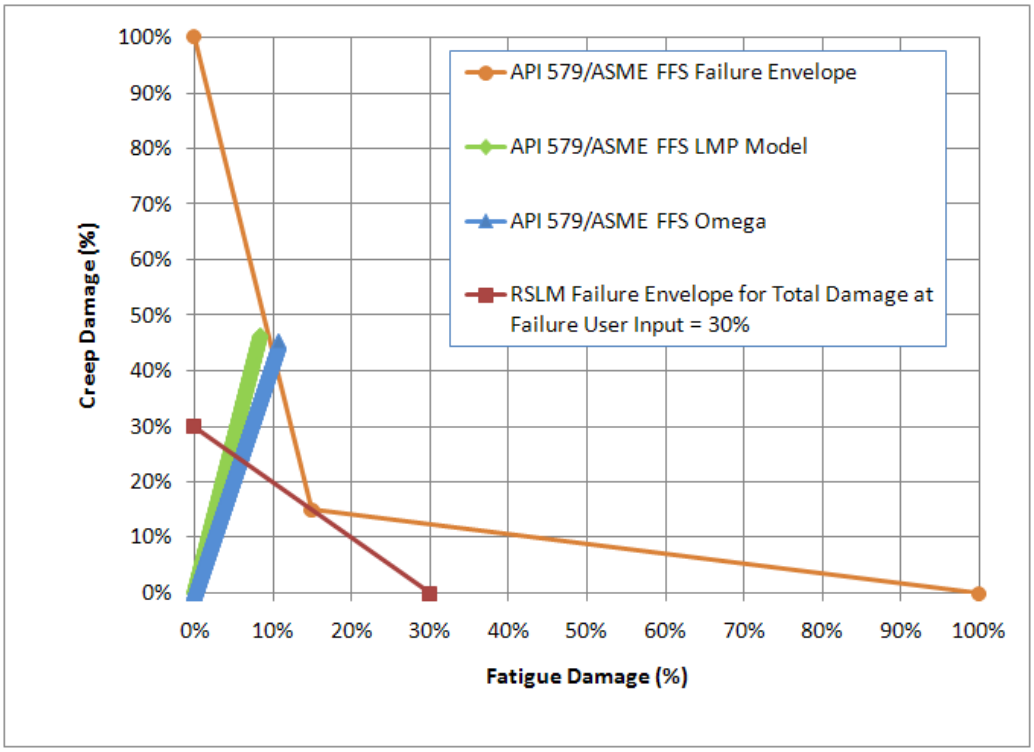

Figure 7-5
Plot of Damage Criterion After Each 300-Hour Load Cycle Until Failure for Creep-Fatigue, Example 1

Observations on Creep-Fatigue Interaction Examples

1. The interaction of creep and fatigue is an important consideration when both modes are present, but there is considerable data scatter and debate regarding the intensity of the interacting effect. However, the linear interaction provided in RLSM is generally not considered to be the correct approach for evaluating creep-fatigue interaction. RLSM's creep-fatigue interaction failure criterion is based on the sum of creep and fatigue damage and a user-entered failure value:

   $D_f + D_c < D_{\text{user failure criteria}}$

   In contrast, API 579/ASME FFS uses the more widely accepted bilinear damage failure envelope shown in Figure 7-2.

2. There is a potential for inconsistency in safety margins. Based on the example problems, it appears that average time to rupture values are to be used and code fatigue curves. The code fatigue curves provide a significant design factor, whereas the average rupture properties do not. Guidance on design factors should be provided to the user.

8
CREEP-FATIGUE CRACK GROWTH

BLESS Creep Crack Growth Methodology

The Boiler Life Evaluation and Simulation System (BLESS) is a program licensed by EPRI to evaluate the growth of cracks in headers and pipes. BLESS Version 4.3 was provided for this evaluation. The focus of this study was on the crack growth rate modeling for flaws in pipes. The BLESS program allows the user to perform either a deterministic or probabilistic analysis for calculating the crack growth rate. For purposes of comparison with the API 579/ASME FFS methodology, the project team analyzed only the deterministic approach and set all secondary variables to zero.

The overall approach in BLESS is similar to ASME Section XI, Section VIII, Division 3 and API 579/ASME FFS in that FEA was used to develop new geometry modification factors. This approach was used in spite of the fact that the Buchalet and Bamford stress intensity solutions [13] had been available for over 20 years and were used in Section XI and Division 3.

The BLESS program allows the user to enter the system geometry, including pipe dimensions and crack orientation. The user can specify a continuous axial or circumferential crack as buried, ID connected, or OD connected. If a semi-elliptical crack is chosen, the user is allowed only to specify ID connected for both an axial and a circumferential crack. BLESS's primary calculation for crack growth is the following equation:

$$\Delta a_{cycle} = C_f \Delta K^{n_f} + t_f C_c \left(C_{t(ave)}\right)^{n_c}$$

The BLESS program literature references several sources as the basis for K_I, the stress intensity factor, and C_t, the time-based crack driving force, used for fatigue and creep crack growth, respectively. the project team reviewed Zahoor [11] and Kumar [12], the BLESS sources for the fatigue-based infinite length axial crack growth expressions and creep crack growth relations, respectively. In order to compare BLESS results with those of API 579-1/ASME FFS-1, the project team analyzed an infinite length axial flaw and followed the procedure in the referenced papers that BLESS documents for developing the K and C* values for such a geometry. Appendix C documents the equations for the K_I value as the crack grows through the thickness of the pipe according to the referenced paper. The referenced source [11] for the axial and circumferential continuous flaws addresses only ID-connected (inner surface) flaws. However, the BLESS documentation indicates that it uses the same methodology for OD-connected (outer surface) flaws, and this was confirmed by running identical conditions for ID and OD cracks and obtaining the same results.

The documented references for K_I and C* values mention a range of R/t of 5–20 (where R is the outer radius and t is the wall thickness); however, the BLESS program allows users to analyze geometries outside that range without producing any apparent warning. This lack of warning when the user is out of range is a potential pitfall for novice users of BLESS.

The BLESS program calculates the stresses used for the fatigue and creep crack growth rate equations based on an operating history of pressure and an axial stress. The BLESS output displays cyclic stresses that are equivalent to Pr/t_w and $Pr/(2t_w)$, where Pr is the pressure (radial) and t_w is the wall thickness for homogeneous material, for the hoop and axial stresses, respectively. The project team was able to recreate BLESS's calculated fatigue-only da/dt using the displayed cyclic stresses. (Typically, for fatigue calculations da/dN is calculated, but it can easily be converted to a time-based derivative to compare with BLESS output.) This is in contrast to the stress formula found in Zahoor [11], which is the BLESS referenced source for the stress intensity factor for the analyzed geometry. The stress formula recommended by Zahoor produces a higher stress than the formulation that BLESS uses.

Despite being able to benchmark the da/dt calculation for a pure fatigue analysis, the project team was unable to match the corresponding reported crack dimensions. BLESS produced a larger crack dimension at each time step than what the reported or calculated da/dt would suggest. For example, Table 8-1 shows that between 1,950,000 hours and 1,980,000 hours the crack grew from 0.12293 to 0.12544 inches; this is an effective da/dt of 9.96E-8, which is higher than the da/dt reported at any of the time periods listed in the table.

Figure 8-1 compares the crack depth over time reported by BLESS with the calculated crack depth derived from the project team's understanding of the BLESS algorithms [11], which show a higher than expected crack growth rate. It is probable that since BLESS was not intended to operate in the fatigue-only range, it has not been validated for such cases.

In conclusion, there are a few aspects of BLESS that could result in nonconservative answers; however, there also appears to be an adjustment factor of some type that accelerates the crack growth rate. The stress formulation of pr/t and pr/2t, where r is the inner radius, is a nonconservative estimate of the hoop and longitudinal stresses. Additionally BLESS does not check FAD criteria, which means that it overlooks potential failures before a through-thickness crack. While BLESS allows for a defined failure point before a through-thickness crack, checking FAD criteria requires checking at each iteration of the fracture mechanics process. Another potential source of nonconservatism is that BLESS does not explicitly state during operation of the program that the R/t range is 5–20 for valid solutions, and it allows for the solution of geometries outside that range. Finally there appears to be some additional adjustment factor that reintroduces conservatism into the solution because the crack growth from the output does not appear to match the listed da/dt values.

Table 8-1
BLESS Pure Fatigue Example

a (inches)	Time, t (hrs)	Ct, Ctavg	da/dt
0.12293	1,930,000	5.78E-07	4.79E-08
0.12544	1,950,000	5.99E-07	5.18E-08
0.12813	1,980,000	6.22E-07	5.62E-08
0.13106	2,000,000	6.47E-07	6.13E-08

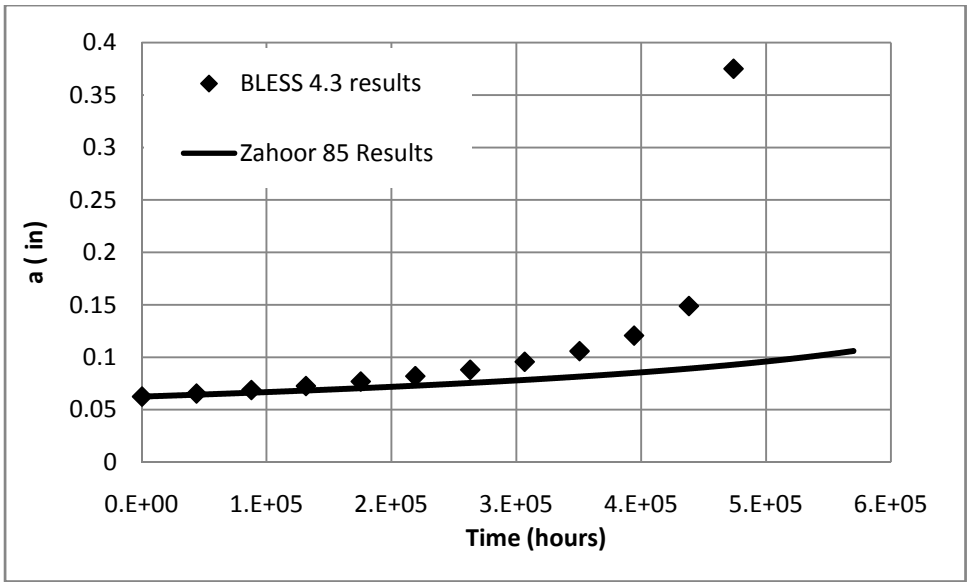

Figure 8-1
Comparison of BLESS 4.3 Results with Calculated Results from Zahoor [11]

API 579/ASME FFS Creep Crack Growth Methodology

Section 10.5.4 of API 579-1/ASME FFS-1 details an analysis procedure to evaluate a component operating in the creep regime with a crack-like flaw using the results from a stress analysis. In contrast with the creep analyses described in Section 5, which rely on a maximum stress value, the creep crack growth method uses the FEA-determined stresses at a point in the wall of the component.

Figure 8-2 depicts a flow chart illustrating the API 579/ASME FFS creep crack growth method. The inputs to the process include the following:

- Component geometry and material
- Initial crack dimensions (a_o, c_o), location and orientation
- Prior creep or fatigue damage
- Operating (load and temperature versus time) cycles
- FEA-determined stress profiles for each operating load condition

The steps for making the operating conditions into discrete units are to divide the operation into load cycles and to further partition each load cycle into time increments for the purpose of summing up time-based damage that occurs during the load cycles. The time-based damage includes the creep damage (time to rupture) that is ahead of the crack growth and the time rate of crack growth ($\frac{da}{dt}$ and $\frac{dc}{dt}$).

These equations (see Appendix B.3) utilize the crack and component geometry-based reference stress solutions from Annex D [1] as the reference stress for time to rupture (see the equations in Appendix B.1) and for evaluating the time-based crack growth driving force. Omega model parameters, accumulated creep and fatigue damage, and the stress intensity factor (which is crack

and component geometry-based) from Annex C [1] are also used in the time-based crack growth model. See Appendix B.3 for a complete listing of these equations. In contrast with BLESS, API 579-1/ASME FFS-1 contains different correlations for ID and OD cracks for the semi-elliptical crack geometry.

Although API 579-1/ASME FFS-1 allows the use of data other than the Omega material model, the only expressions presented use Omega parameters (see Appendix B.3 for these expressions); thus, the most straightforward implementation of API 579-1/ASME FFS-1 is via the Omega material model.

The crack dimensions are updated for each incremental time period. Once the load cycle has been completed, the fatigue-based crack growth is computed based on the equations in Appendix B.4. The user is left to determine the appropriate coefficients for the Paris Law equations ($e.g. \frac{da}{dN} = C\left[\Delta K_{eff}^{0}\right]^{m}$) and the R-ratio effect on the crack growth model. API 579-1/ASME FFS-1 Annex F, Section F.5.3 provides the user with a number of crack growth model equations for different materials and operating conditions. A limited number of crack growth models are included for high-temperature operation.

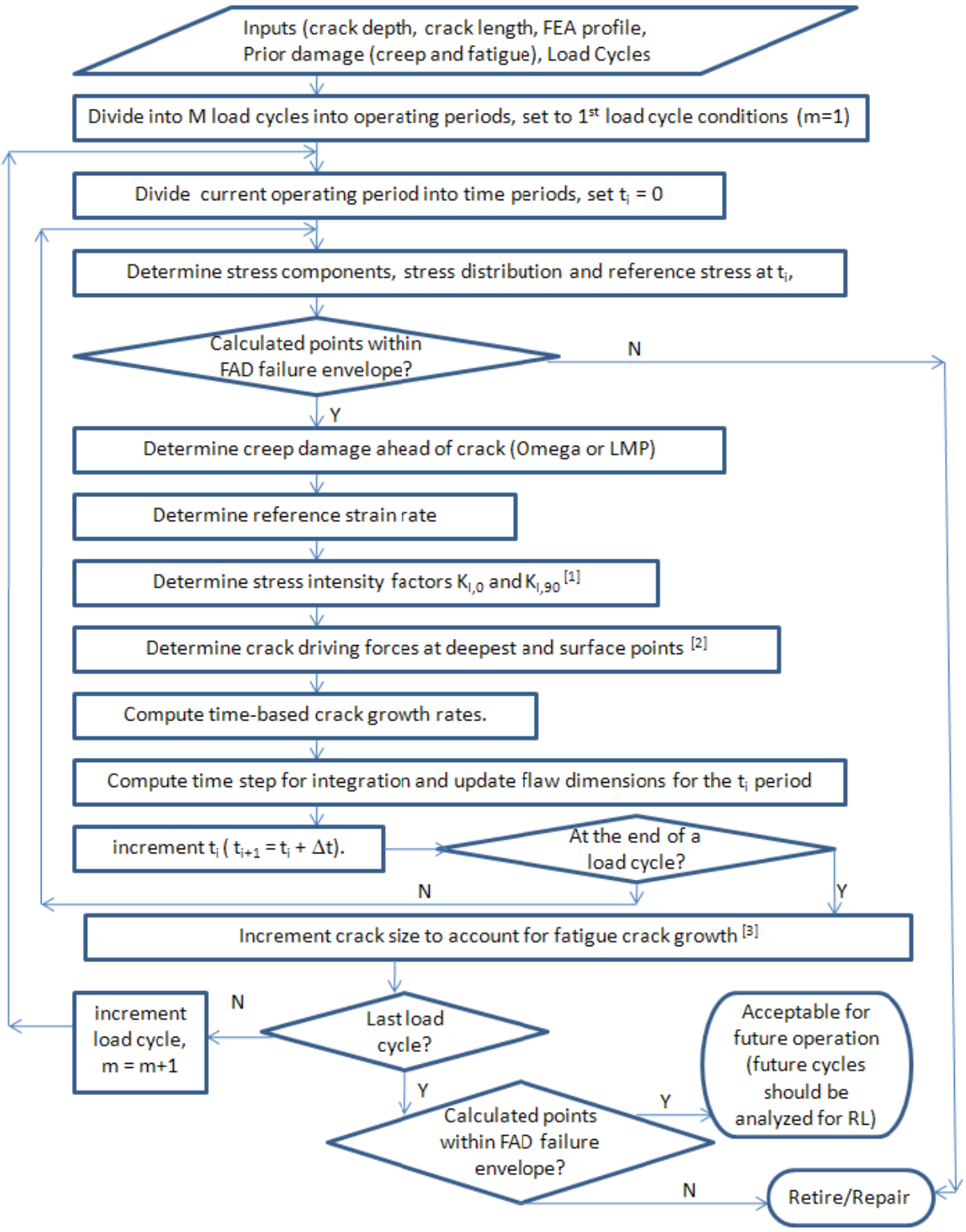

Figure 8-2
API 579/ASME FFS Creep Crack Growth Methodology

Creep Crack Growth Examples

A single component and crack geometry was used for the purposes of comparing the BLESS and API 579-1/ASME FFS-1 creep crack growth methodologies. While circumferential cracks are relevant and have occurred in boiler tubes due to pipe bending, the infinitely long longitudinal crack for a cylindrical component, also a relevant geometry, was selected for these examples.

Simulations using the analysis methodology of Section 10.5.4 as previously described and shown in Figure 8-2 have been performed for the case of an infinite longitudinal crack in a cylinder and then compared with BLESS simulations using identical inputs. The simulation geometry for the examples in this section is shown in Table 8-2.

Table 8-2
Crack and Component Simulation Geometry

Initial Crack Depth (a_o)	0.0625 inches
Pipe Size	15.75 inch OD 0.375 inch wall thickness
Material	2¼ Cr – 1 Mo
Crack description	Surface crack, inside surface, longitudinal direction, Infinite length
Fatigue crack growth factor, C*	1.5E-9
Fatigue crack growth factor, m*	2.87
Annex C [1] relations for stress intensity factor (API 579/ASME FFS simulation)	C.5.11
Annex D [1] relations for reference stress (API 579/ASME FFS simulation)	D.5.11

*These factors were from an example problem in the BLESS supplied database. API 579/ASME FFS Section F.5.3 can also be used as a source of a number of crack growth factors.

Fatigue-Only Example

The geometry listed in Table 8.2 was simulated for a fatigue-only case, with conditions and results described in Table 8.3.

Table 8-3
Fatigue-Only Simulations and Results

Through thickness stress	21,500 psi (uniform)
Fatigue cycle time	240 hours
Temperature	< 100ºF (constant)
BLESS Failure Mode	Through-wall crack
Zahoor [11] Failure Mode*	Through-wall crack
API 579-1/ASME FFS-1 Failure Mode	Outside FAD envelope
BLESS Life Prediction	261 years/9,530 cycles
Zahoor [11] Life Predictions*	424 years/15,476 cycles
API 579-1/ASME FFS-1 Life Prediction	411 years/15,002 cycles

*The expressions in this paper, referenced by BLESS, were used to simulate the crack growth, resulting in different life predictions, presumably owing to a presumed adjustment factor in BLESS.

As previously discussed, API 579-1/ASME FFS-1 contains correlations for both inside and outside surface cracks for all cylindrical and spherical components. Figure 8-3 shows that for the examples considered, there is no significant difference in the time to failure for these geometries. However, it is important to note that there are likely operating conditions where differences in crack location would produce important differences in life estimates.

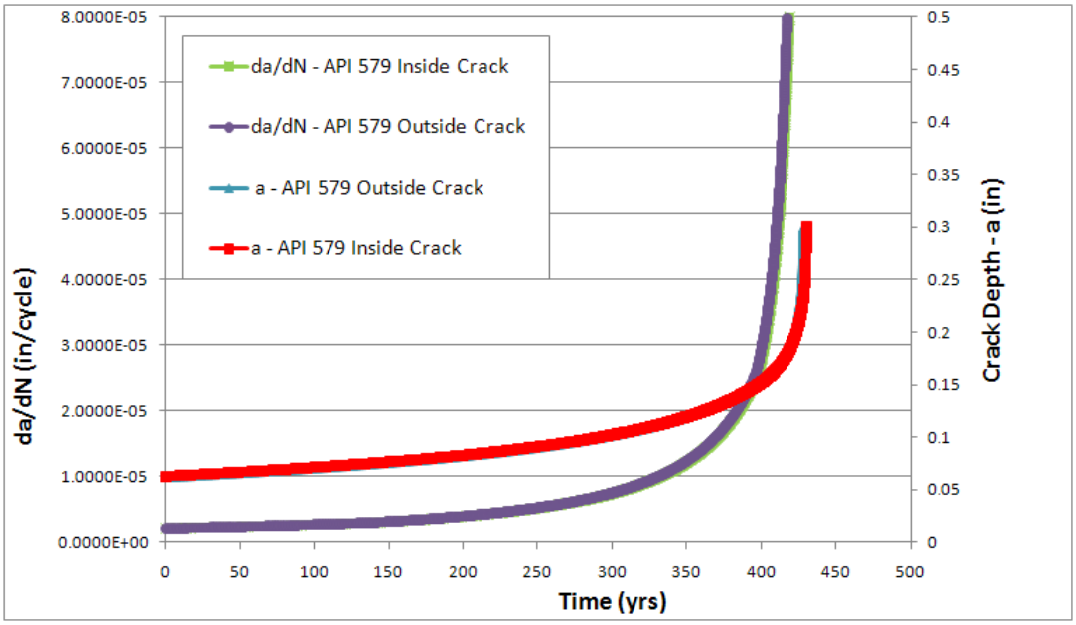

Figure 8-3
Comparison of Fatigue-Only Crack Growth Rate (da/dN) and Crack Depth (a) Using API 579/ASME FFS for Inside and Outside Surface Cracks; Curves for Inside and Outside Cracks Fall on Top of Each Other

For the API 579-1/ASME FFS-1 simulation, the failure was via operation outside the failure analysis diagram (FAD) envelope. For the BLESS simulation, the component failed as a result of reaching through wall thickness. Figure 8-4 shows the FAD diagram for the outside crack case simulated via API 579-1/ASME FFS-1.

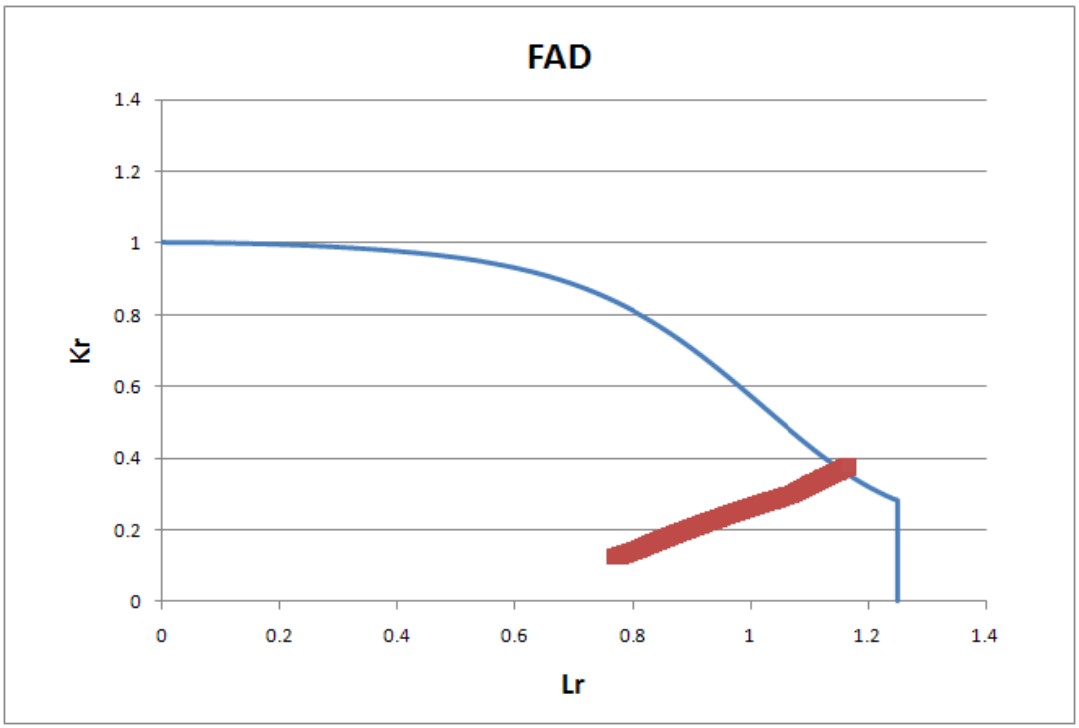

Figure 8-4
FAD Envelope for the Fatigue-Only Example

BLESS reports fatigue cycle damage in terms of time, or da/dt. Figures 8-5 through 8-7 compare the BLESS da/dt for this example with the initial portion of the API 579-1/ASME FFS-1 simulation, with the latter's crack growth rates converted to da/dt for comparative purposes.

Note that all three simulations agree in the early part time portion, but Figures 8-5 and 8-6 show that both the BLESS crack growth rate and crack depth increases much faster than the other simulations after 100 years. As previously reported, the project team has not been able to reverse calculate the BLESS reported crack depth, in spite of BLESS reporting da/dt and time increment values. The "enhancement" of crack depth causes the crack growth rate to accelerate.

Figure 8-7 shows that all models are using similar stress intensity factor relations. The BLESS failure mode is a user-specified percent through-wall value, while the API 579-1/ASME FFS-1 simulation failure mode is via breaching of the FAD envelope.

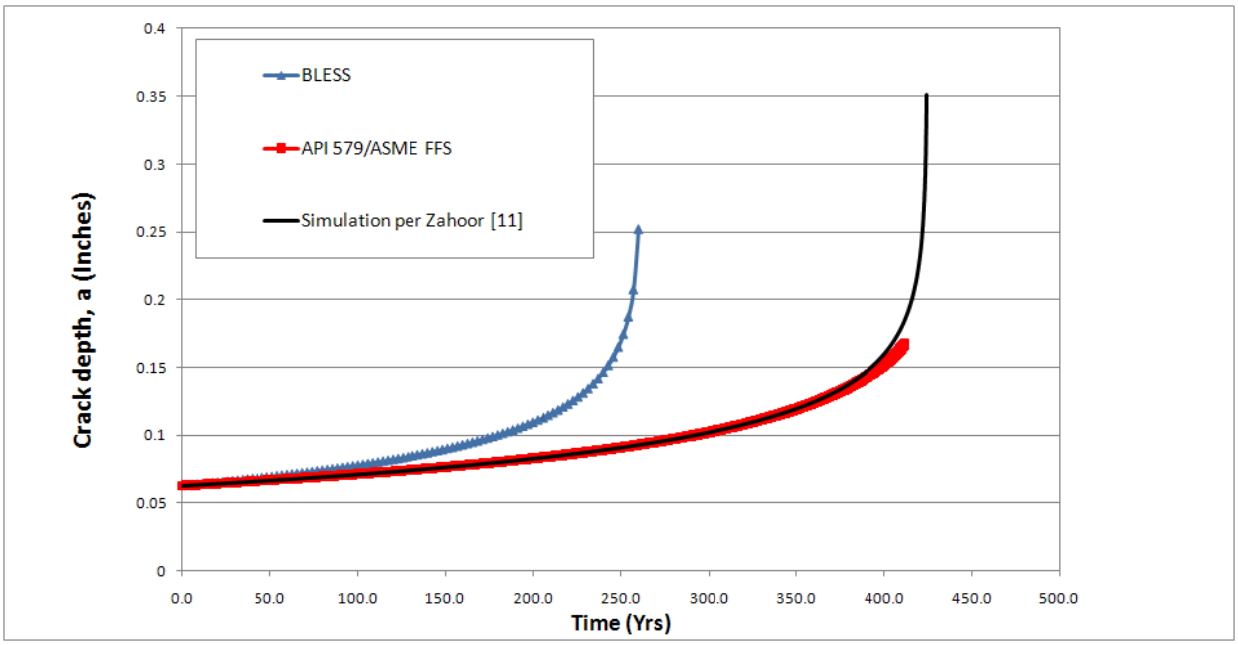

Figure 8-5
BLESS, Zahoor Expressions [11], and API 579-1/ASME FFS-1 Fatigue-Only Crack Depth over Time Comparison

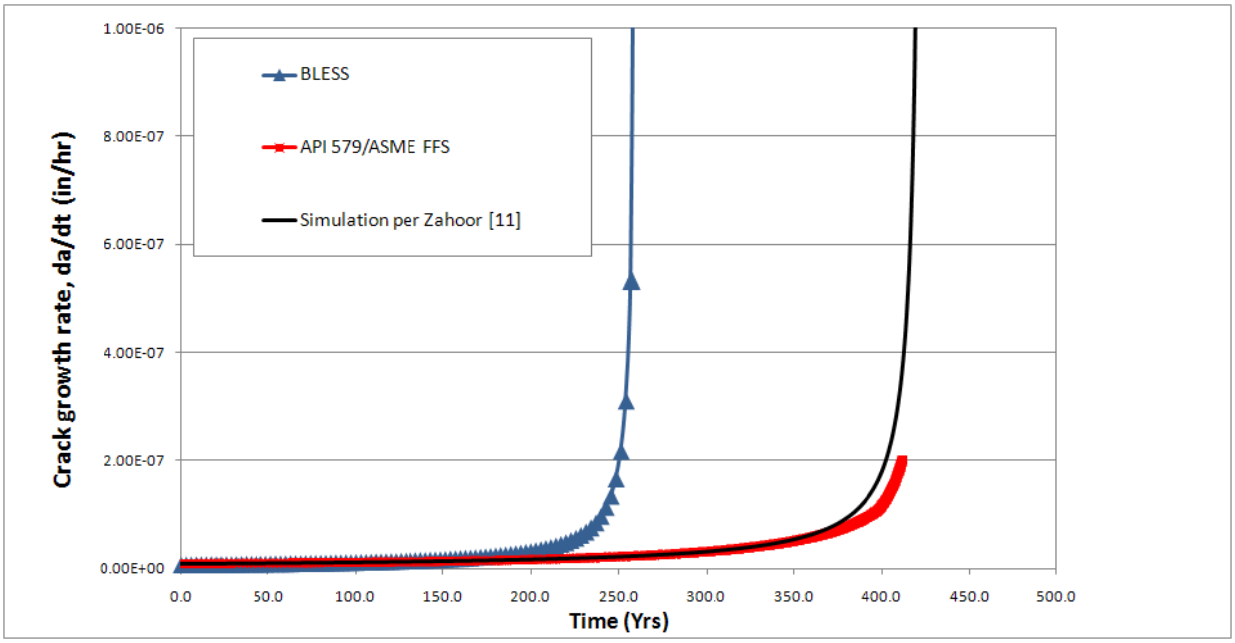

Figure 8-6
BLESS, Zahoor Expressions [11], and API 579-1/ASME FFS-1 Fatigue-Only Crack Growth Rate over Time Comparison

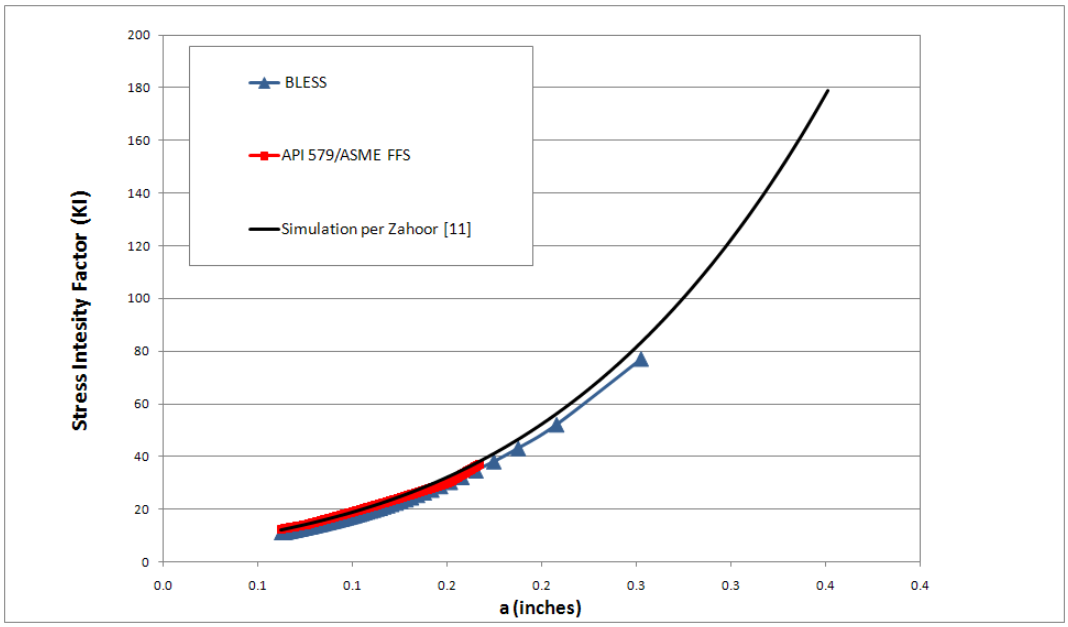

Figure 8-7
BLESS, Zahoor Expressions [11], and API 579-1/ASME FFS-1 Fatigue-Only Stress Intensity Factor as a Function of Crack Depth; BLESS K_I Not Reported, But Reverse Calculated

Creep-Only Example

The geometry listed in Table 8-2 was simulated for a creep-only case. The conditions and results of this simulation are described in Table 8-4. The through-wall stress thickness was selected to be uniform and near the allowable stress. In modeling creep crack growth rates, the following formula applies to both models assessed:

$$da/_{dt} = C_c \, C_t^{n_c}$$

In the case of the API-579/ASME FFS approach, the C_c and n_c parameters are derived from the Omega material model parameters or:

$$C_c = \Omega/_{500}$$

$$n_c = n_{BN}/_{(n_{BN}+1)}$$

For the simple example simulated, since effective stress and temperature remained constant, these factors are constant. The BLESS simulation conducted included using these values so that the factors for the two simulations were identical.

Table 8-4
Creep-Only Simulation and Results

Through thickness stress	8,000 psi (uniform)
Fatigue cycle time	2,000 years (i.e. no fatigue)
Temperature	1000°F (constant)
C_{creep}	0.05585
n_{creep}	0.907
BLESS Failure Mode	Through-wall crack
API 579/ASME FFS Failure Mode	Accumulated creep damage reaches 80%
BLESS Life Prediction	9.9 years
API 579/ASME FFS Life Prediction	24 years

Figures 8-6 and 8-7 compare the creep crack growth rates and crack depth over time, respectively, predicted by the two models. As in the fatigue life example, there are notable differences, with BLESS reporting a through-wall crack at 9.9 years and API 579-1/ASME FFS-1 requiring repair or replacement at 24 years due to the component reaching an accumulated creep damage of 80%. The creep crack driving force is plotted in Figure 8-8 versus the crack depth. BLESS's computed crack driving force is larger for small crack depth, causing faster crack growth in this model. Figure 8-9 shows the accumulated creep damage profile for the API 579/ASME FFS simulation. The project team was able to recreate all BLESS results, including incremental crack depth, by implementing the methodology outlined in Kumar [12].

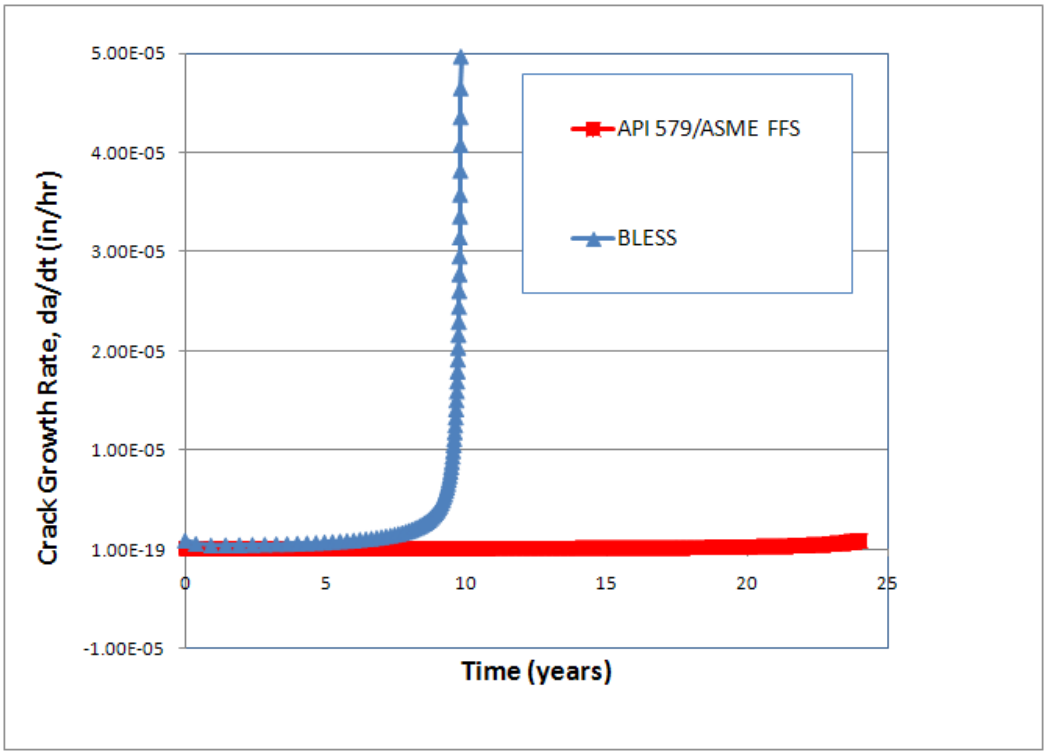

Figure 8-6
BLESS and API 579-1/ASME FFS-1 Creep-Only Comparison of Crack Growth Rates over Time

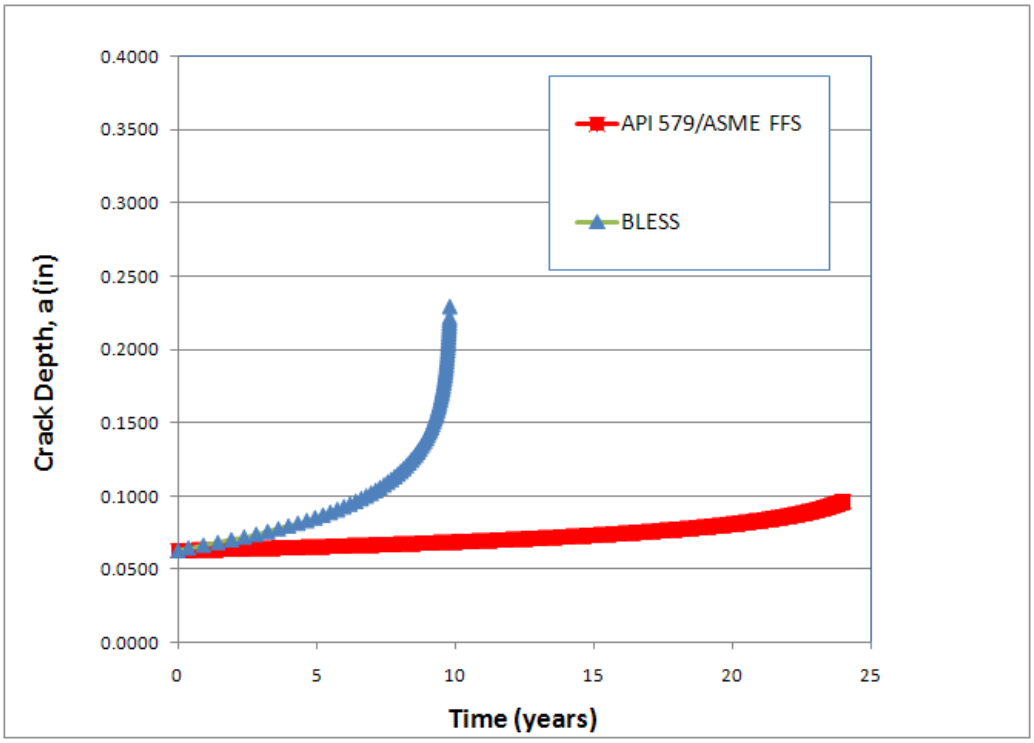

Figure 8-7
BLESS and API 579-1/ASME FFS-1 Creep-Only Comparison of Crack Depth over Time

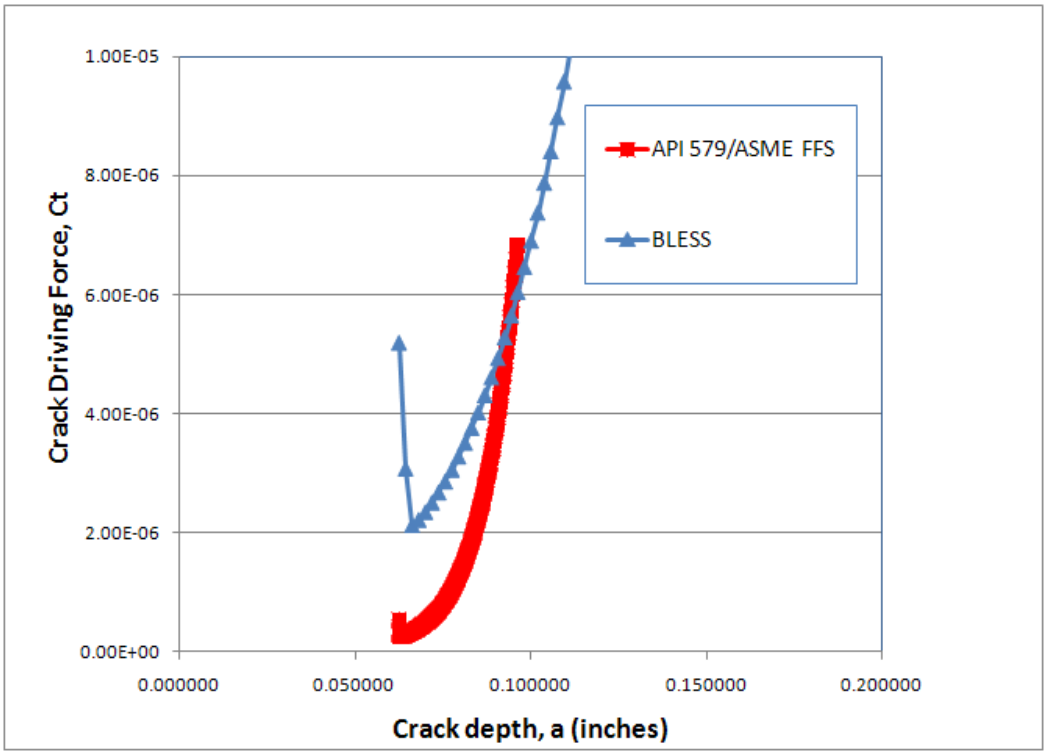

Figure 8-8
BLESS and API 579-1/ASME FFS-1 Creep-Only Comparison of Crack Driving Force as a Function of Crack Depth (a)

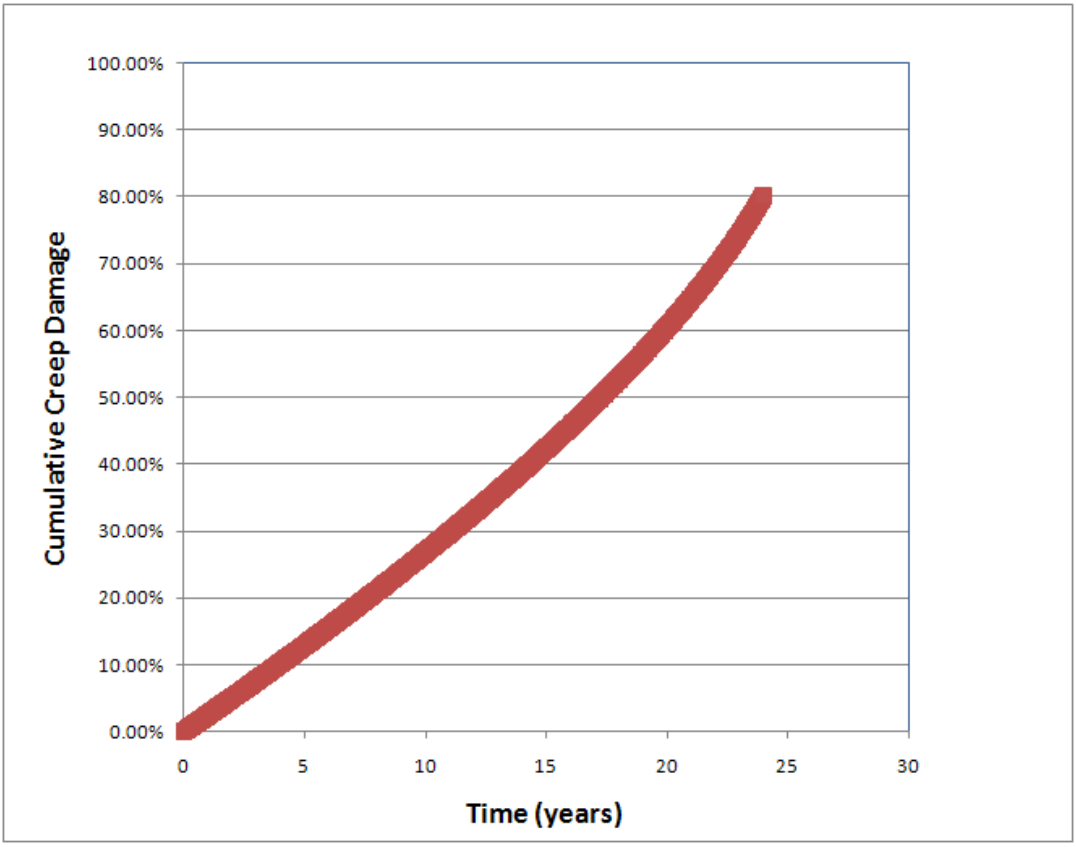

Figure 8-9
Accumulated Creep Damage for API 579/ASME FFS Model Simulation; Repair or Replacement Is Required at 80% Damage

Observations on Creep Crack Growth Examples

The major conclusion arising from these examples is that the two models are capable of producing very different life predictions for both fatigue and creep crack growth. In the case of fatigue, the stress intensity factors for the geometry considered—an infinite longitudinal crack in a cylindrical component—were in close agreement. The crack incrementation schemes were different, producing different component lives. In addition, failures occurred for different reasons.

For the simple creep-only example for the same geometry, different creep crack growth driving forces primarily contributed to the difference in remaining life. Again, the failure reasons were different.

The API 579/ASME FFS is more versatile than the BLESS model, allowing consideration of multidimensional stress states and stress profiles in the component wall.

9
CONCLUSIONS

RLSM and API 579-1/ASME FFS-1 have many common features in modeling creep and fatigue. The results produced by an API 579-1/ASME FFS-1 assessment can be matched in many cases through user-entered material data. In some cases, matching the results is cumbersome.

The inclusion of creep relaxation effects would be an important addition to the version of RLSM studied in this evaluation. A beta version of RLSM does exist that includes creep relaxation, but there are no current plans to finalize and issue this software. The accurate modeling of creep relaxation can eliminate a significant amount of excessive conservatism, particularly if the creep-fatigue monitoring program is being installed in a new plant. Note that simulation of creep relaxation in a real piping system is not straightforward.

In general, RLSM requires an experienced user to set up a new plant. If it is desired to broaden the RLSM user base, a number of steps could be undertaken to improve usability. The first step would be inclusion of significantly more material data, including fatigue and creep models. EPRI has a large effort ongoing in developing creep fatigue material information for Grades 11, 22, and 91 and for austenitic stainless steel materials. When complete, it is planned that this information will be included in RLSM.

Until that project is completed, material data in API 579-1/ASME FFS-1 or Subsection NH could be used for high-temperature fatigue curves. API 579-1/ASME FFS-1 Omega and LMP creep time to rupture material models could be incorporated as well. In order to include these other types of fatigue and creep modeling methods, a larger variety of stress states should be included for each location. This could include providing correlations for von Mises and maximum principal stress so that the user could compare and contrast results using a variety of methods for every location. In this scenario, there would be more user-friendly drop-down controls listing available material models and options, each including a reference to the appropriate code basis. The ability to enter new data and update old data should be provided, or an interface could be established with a license server that includes the latest code changes. With the inclusion of all these options, there should also be clear warnings about the incorrect mixing of certain stress basis and fatigue/creep modeling methods. For example, if a user were to inadvertently use B31.1 stresses with a smooth bar fatigue curve, the resulting calculated fatigue life would be significantly nonconservative.

The combination of creep and fatigue damage should be made more sophisticated to allow the inclusion of a non-linear creep-fatigue damage envelope. The current handling of creep-fatigue interaction in RLSM is not considered completely correct and can be either overly conservative (if total allowable damage is set to 0.3), or nonconservative (if total allowable damage is set to 1). Note that the best method of modeling creep-fatigue interaction is a controversial and unresolved topic, and no recommendation is made at this time with respect to the best approach. Hopefully, when the above referenced project is completed, this issue will be resolved.

Some significant discrepancies between the Omega and LMP material data for 9 Cr – 1 Mo were found. These discrepancies were identified to be in the extrapolated range or in regions where no rupture data existed. API 579/ASME FFS does not specify valid use ranges for the Omega material model, and this represents a potential pitfall for the novice user of API 579/ASME FFS. This is a very important future enhancement for API 579/ASME FFS in order to prevent inaccurate creep rupture predictions.

For the creep crack growth comparison, large differences were found in life estimates and failure mode for both fatigue and creep. BLESS predicted far shorter lives than API 579/ASME FFS for the examples studied and can be considered more conservative. For fatigue crack growth, the incremental crack depth scheme appears to have an internal adjustment factor to accelerate the crack growth rate. This adjustment factor was observed for the fatigue-only example and not in the creep-only example. This adjustment factor should be explained to the user, or if it is a program error, it should be corrected. For creep crack growth, the major factor affecting the models' differences appears to be due to the relations for crack driving force. BLESS uses a stress basis of pr/t and pr/2t for hoop and axial stresses where r is the inner radius. The project team recommends to switch the stress basis to that of the reference papers, to use the outer radius not the inner radius, or to use thick-walled cylinder equations. Additionally, it is recommend to warn the user if the geometry of the problem being analyzed is outside the R/t range of 5–20, which is listed as the limit of the range of applicability by the reference papers.

BLESS predicts failure based on the user-specified percent of wall thickness penetrated by the growing crack. In contrast, the API 579/ASME FFS method has required additional checks for operation outside the FAD envelope and accumulated creep and fatigue damage as criteria for repair and/or replacement. This is a more comprehensive check on failure and should be a future BLESS enhancement.

In general, although methods identified on how each assessment type addresses damage initiation and growth, methods within the EPRI software have been shown to be more conservative than API 579/ASME FFS methods. The user is cautioned to understand where this is true and where more conservative analysis is warranted. Materials information improvements were also identified, many of which are the subject of ongoing work within EPRI's creep strength enhanced ferritics steels project and the EPRI creep fatigue project. As data are developed, this information will be incorporated into the software codes.

10
NOMENCLATURE

a	Crack depth (in)
c	Crack half length (in)
CLMP	Larson Miller constant
C_c	Creep crack growth rate factor
C_f	Fatigue crack growth rate factor
D_c	Creep damage
D_f	Fatigue damage
K_I	Stress intensity factor
D_f	Fatigue damage
L_r	Load ratio
K_r	Stress intensity ratio
n_c	Creep crack growth rate factor
n_f	Fatigue crack growth rate factor
N_{fi}	Number of fatigue cycles to retirement
P	Pressure (ksi)
r	Inner radius (in)
R	Outer radius (in)
t_w	Wall thickness (in)
t	Time (hours)
T_{RI}	Time to rupture for period i
$\dot{\varepsilon}_{co}$	Initial creep strain rate
$\dot{\varepsilon}_c$	Creep strain rate
ε_{co}	Creep strain
Ω	Omega
$\bar{\sigma}$ =	Stress
ΔK	Stress intensity factor range

11
REFERENCES

1. API 579-1/ASME FFS-1, 2007 Edition.
2. Phone conversation with Structural Integrity Associates Engineers on November 11, 2009.
3. Creep-FatiguePro Technical Documentation.
4. ANSI/ASME B31.1-2007.
5. M. Prager, S. Ibarra, "Approaches to Long Term Life Prediction of Furnace and Boiler Tubes," Fitness for Adverse Environments in Petroleum and Power Equipment, ASME PVP. Vol. 359, 1997, pp. 339–352.
6. M. Prager, "Modeling multiaxial creep and damage for application to pressure vessels and piping," paper presented at the Symposium of Inelasticity and Damage in Solids Subject to Microstructural Change, Memorial University, Sept 25–27, 1996.
7. W. J. Koves, "Comparison Pressure Vessel and Piping Fatigue Criteria," paper presented at the ASME Pressure Vessel and Piping Conference, 88-PVP-5, June 1988.
8. 2004 ASME Boiler and Pressure Vessel Code Section III, Subsection NB.
9. ASME Boiler and Pressure Vessel Code Section III, Subsection NH.
10. Private communications with Structural Integrity Associates on December 10, 2009.
11. A. Zahoor. "Closed Form Expressions for Fracture Mechanics Analysis for Cracked Pipes," *Journal of Pressure Vessel Technology*, Vol. 107, 1985, pp. 203–215.
12. *An Engineering Approach for Elastic-Plastic Fracture Mechanics.* EPRI, Palo Alto, CA: 1981. NP-1931.
13. C. B. Buchalet and W. H. Bamford, "Stress Intensity Factor Solutions for Continuous Surface Flaws in Reactor Pressure Vessels, Mechanics for Crack Growth." ASTM STP, 590, 1976: pp. 385–402.
14. Private communications with David Osage and Martin Prager, February 2010.
15. T. L. Anderson and G. Glinka, "A Closed-Form Method for Integrating Weight Functions for Part-Through Cracks Subject to Mode I Loading," Engineering Fracture Mechanics, Volume 73, Issue 15, October 2006.
16. Private communication with SIA, March 2010.
17. ANSI/API RP-530, 2003 Edition.

A
BENCHMARKS

A.1 RLSM Creep Damage Accumulation Routine

This benchmark was performed to validate the project team's understanding of RLSM's creep time to rupture methodology. A total of four 2,000-hour test cases were performed using RLSM. For all the test cases, temperature and pressure were held constant at 1100ºF and 1730 psi, and no other loads were included beyond internal pressure. The results are shown in Tables A-1 through A-4, where Table A-1 uses thick wall stress correlations; Table A-2 uses thin wall stress correlations; Table A-3 uses the thick wall stress correlation for hoop stress, but sets the axial stress equal to the radial stress (that is, negative); and Table A-4 sets the axial stress equal to what the equivalent Tresca stress would be at the inner diameter of the pipe. The goal of this benchmark was to recreate the RLSM results with manual/spreadsheet calculations. The project team was able to do so using the LMP formulation of Equation 5-1 and the LMP coefficients in the RLSM test cases' databases. These tests confirmed the following:

1. RLSM uses the maximum principal stress.
2. RLSM uses the LMP formulation found in Section 5.1

Table A-1
Test Case 1, σ_h = 2.904575 x Internal Pressure, σ_a = 0.952287 x Internal Pressure (thick walled equation)

Time	avg T (ºF)	Avg P (psi)	Stress Displayed by RLSM (ksi)	Creep Damage
11/1/2009 23:30	1100	1730	5.024915	0
1/24/2010 23:30	1100	1730	5.024915	0.009258178

Table A-2
Test Case 2, σ_h = 2.815789 x Internal Pressure, σ_a = 1.407895 x Internal Pressure

Time	avg T (ºF)	Avg P (psi)	Stress Displayed by RLSM (ksi)	Creep Damage
11/1/2009 23:30	1100	1730	2.435658	0
1/24/2010 23:30	1100	1730	2.435658	0.007797494

Table A-3
Test Case 3, □h = 2.904575 x Internal Pressure, □a = -1.0 x Internal Pressure

Time	avg T (ºF)	Avg P (psi)	Stress Displayed by RLSM (ksi)	Creep Damage
11/1/2009 23:30	1100	1730	5.024915	0
1/24/2010 23:30	1100	1730	5.024915	0.009258178

Table A-4
Test Case 4, □h = 0.0 x Internal Pressure, □a = 3.904575 x Internal Pressure

Time	avg T (ºF)	avg P (psi)	Stress Displayed by RLSM (ksi)	Creep Damage
11/1/2009 23:30	1100	1730	6.754915	0
1/24/2010 23:30	1100	1730	6.754915	0.05079135

A.2 RLSM Fatigue Damage Accumulation Routine

This benchmark tested the project team's understanding of RLSM's fatigue damage accumulation routine. A single test case was run in which the pressure varied from 0 psi to 964 psi and the temperature ranged from 70ºF to 650ºF, with a total cycle time of 20 hours. Figure A-1 shows a plot of the damage accumulation and the temperature pressure swings. The axial stress equaled 67.95 times the temperature plus 1.407895 times the pressure, and the hoop stress was equal to 2.904575 times the pressure.

After mimicking RLSM's rounding method, the RLSM damage prediction was still 8% higher than the project team's fatigue damage calculations. This is most likely due to RLSM's inclusion of thermal stresses.

This test confirmed the following:

1. RLSM uses the maximum principal stress for fatigue damage calculation.
2. RLSM rounds to integer values and uses a log-log interpolation of whichever fatigue curve is included in the database file.

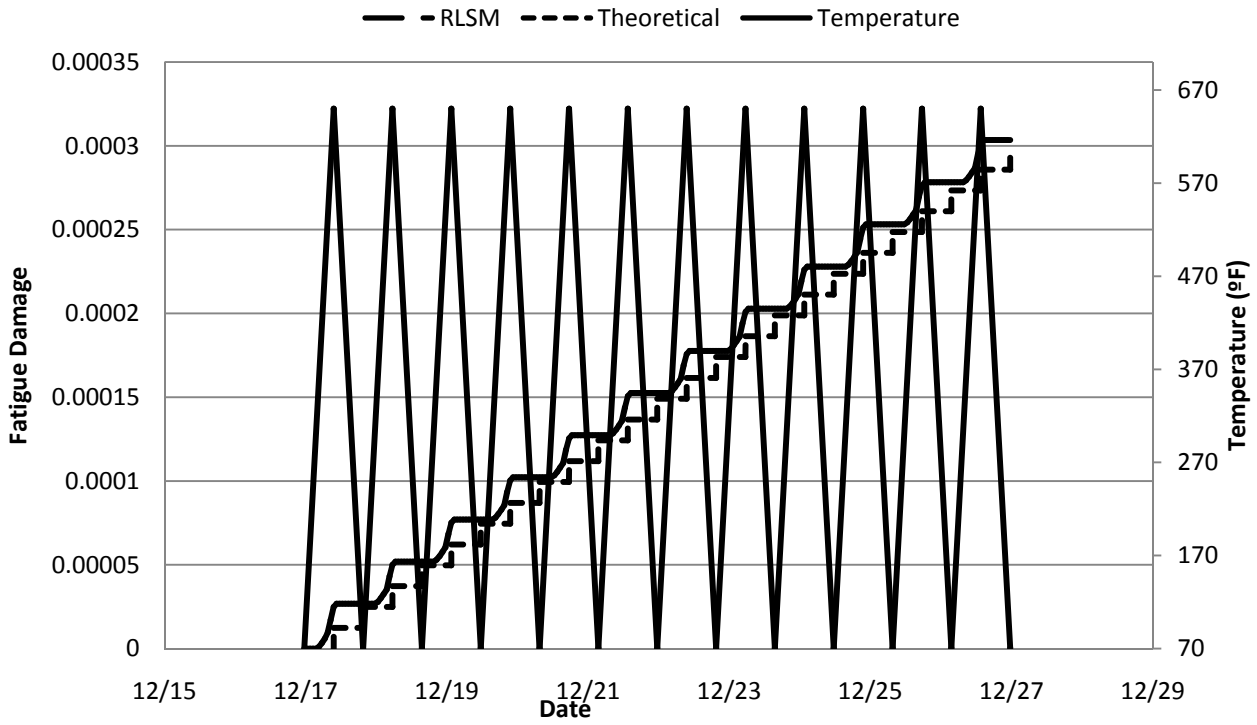

Figure A-1
Damage Accumulation Plot for a Given Temperature Cycle Using RLSM and Hand-Calculated Smooth Bar Fatigue Method

A.3 RLSM Creep-Fatigue Interaction Benchmark

This benchmark was performed to confirm the project team's understanding of how RLSM handled accumulation of damage from both fatigue and creep. The test was conducted for 2-1/4 Cr – 1 Mo steel, with high-temperature fatigue data from Fig. T-1420-1D of Subsection NH [9] and RLSM LMP correlations as listed in Table A-5. The operating conditions were the same as listed in Section 7.3. The plant ran at 70ºF and no pressure for 10 hours, and then had a 10-hour ramp up to 1100ºF and 978 psi with a 270-hour hold time before a 10-hour ramp down to ambient conditions. The axial stress for fatigue was equal to 39.67 times the temperature plus 1.407895 times the pressure, and the hoop stress was equal to 2.904575 times the pressure. The axial stress for creep was equal to 1.407895 times the internal pressure, and the creep hoop stress was equal to 2.904575 times the internal pressure. A summary of differences for damage accumulation for each 300-hour cycle is shown in Table A-6.

RLSM predicted an accumulation of creep damage equal to 1.057115E-4 and an accumulation of 3.007871E-5 fatigue damage for every 300-hour cycle. The calculated amount of fatigue damage exceeds a hand calculation based on the log-log interpolation of Fig. T-1420-1D by approximately 8% which is similar to what Appendix A.2 shows. However RLSM's predicted fatigue accumulation exceeds the API 579 curve fits based on Fig. T-1420-1D by 21%. This implies that the API 579 curve fits can be slightly nonconservative for some ranges of stress.

The amount of creep damage accumulation that the API 579 method predicts is 1.1597E-4. The difference between RLSM and the API 579 calculation is most likely due to the imprecise second order polynomial curve fit that was applied to the API 579 data. This curve fit was used to calculate the correct coefficients for the RLSM database.

The total damage is then added up and compared to the allowable damage, which in this example was set to 0.30. RLSM therefore predicted a life of 2,208 cycles of 300 hours, which is far less than the API 579 prediction. This is because API 579 uses the creep-fatigue damage envelope, which allows the sum of the two damage types to exceed 0.30 as long as one of the damage types is sufficiently low.

Table A-5
RLSM LMP Coefficients to Match API 579 2-1/4 Cr – 1 Mo Data

RLSM LMP Coefficient	Value
C_0	42341
C_1	-1679
C_2	-1746.2

Table A-6
Summary of Differences for Damage Accumulation for Each 300-Hour Cycle

	RLSM	API 579
Creep Damage	1.057115E-4	1.1597E-4
Fatigue Damage	3.007871E-5	2.485E-5

B
API 579-1/ASME FFS-1, 2007 EDITION EQUATIONS

B.1 MPC Project Omega Time to Rupture Equations

$$ {}^{n}T_{r,i} = \frac{1}{\dot{\varepsilon}_{co}\Omega_m} $$

$$ log_{10}\dot{\varepsilon}_{co} = -\left\{(A_o + \Delta_{\Omega}^{n}) + \left[\frac{1}{460 + {}^{n}T}\right][A_1 + A_2 S_l + A_3 S_l^2 + A_4 S_l^3]\right\} $$

$$ \Omega_m = \Omega_n^{\delta_{\Omega}+1} + a_{\Omega} \cdot n_{BN} $$

$$ \Omega_n = \max\ [(\Omega - n_{BN}), 3.0] $$

$$ log_{10}\Omega = \left(B_0 + \Delta_{\Omega}^{cd}\right) + \left[\frac{1}{460 + {}^{n}T}\right][B_1 + B_2 S_l + B_3 S_l^2 + B_4 S_l^3] $$

$$ \delta_{\Omega} = \beta_{\Omega}\left(\frac{{}^{n}\sigma_1 + {}^{n}\sigma_2 + {}^{n}\sigma_3}{{}^{n}\sigma_e} - 1.0\right) $$

$$ n_{BN} = -\left\{\left[\frac{1}{460 + {}^{n}T}\right][A_2 + 2A_3 S_l + 3A_4 S_l^2]\right\} $$

$$ S_l = log_{10}({}^{n}\sigma_e) $$

Note: ${}^{n}\sigma_e$ is the Von-Mises stress, except in the case of creep crack growth analysis, where it is the reference stress according to Annex D.

B.2 Larson Miller Parameter Time to Rupture Equations

$$ log_{10}\,{}^{n}T_{r,i} = \frac{1000 \cdot LMP({}^{n}S_{eff})}{({}^{n}T + 460)} - C_{LMP} $$

$$ {}^{n}S_{eff} = {}^{n}\sigma_e \cdot exp\left[0.24\left(\frac{J_1}{S_s} - 1\right)\right] $$

$$ J_1 = {}^{n}\sigma_1 + {}^{n}\sigma_2 + {}^{n}\sigma_3 $$

$$ S_s = ({}^{n}\sigma_1^2 + {}^{n}\sigma_2^2 + {}^{n}\sigma_3^2)^{.5} $$

Note: ${}^{n}\sigma_e$ is the Von-Mises stress.

B.3 Creep (Time-Dependent) Crack Driving Force Correlations

$$C_t^{90}({}^i a,\ {}^i c) = C^{*90}({}^i a,\ {}^i c)\cdot\left[\left(\frac{t_{relax}^{90}({}^i a,\ {}^i c)}{{}^i t}\right)^{\frac{n_{BN}-3}{n_{BN}-1}}+1\right]$$

$$C^{*90}({}^i a,\ {}^i c) = \left(\frac{{}^i\dot{\varepsilon}_{ref}}{1-D_{bc}-\ {}^i D_{ac}}\right)\frac{\left(K_I^{90}({}^i a,\ {}^i c)\right)^2}{{}^i\sigma_{ref}}$$

$$t_{relax}^{90}({}^i a,\ {}^i c) = \frac{0.91\left(K_I^{90}({}^i a,\ {}^i c)\right)^2}{(n_{BN}+1)\cdot E_y\cdot C^{*90}({}^i a,\ {}^i c)}$$

$$C_t^{0}({}^i a,\ {}^i c) = C^{*0}({}^i a,\ {}^i c)\cdot\left[\left(\frac{t_{relax}^{0}({}^i a,\ {}^i c)}{{}^i t}\right)^{\frac{n_{BN}-3}{n_{BN}-1}}+1\right]$$

$$C^{*0}({}^i a,\ {}^i c) = \left(\frac{{}^i\dot{\varepsilon}_{ref}}{1-D_{bc}-\ {}^i D_{ac}}\right)\frac{\left(K_I^{0}({}^i a,\ {}^i c)\right)^2}{{}^i\sigma_{ref}}$$

$$t_{relax}^{0}({}^i a,\ {}^i c) = \frac{0.91\left(K_1^{0}({}^i a,\ {}^i c)\right)^2}{(n_{BN}+1)\cdot E_y\cdot C^{*0}({}^i a,\ {}^i c)}$$

B.4 Fatigue Crack Growth Expressions

$${}^i a = {}^i a + \frac{{}^m da}{dN}$$

$${}^i c = {}^i c + \frac{{}^m dc}{dN}$$

$$\frac{{}^m da}{dN} = H_f\left({}^m\Delta K_{eff}^{90}\cdot\frac{E_{amb}}{E_T}\right)^{\lambda}$$

$${}^m\Delta K_{eff}^{90} = q_0\left({}^m K_{l,max}^{90} - {}^m K_{l,min}^{90}\right)$$

$$\frac{{}^m dc}{dN} = H_f\left({}^m\Delta K_{eff}^{0}\cdot\frac{E_{amb}}{E_T}\right)^{\lambda}$$

$${}^m\Delta K_{eff}^{0} = q_0\left({}^m K_{l,max}^{0} - {}^m K_{l,min}^{0}\right)$$

$q_0 = 1$ $\quad$ R ≥ 0

$q_0 = \frac{1-0.5R}{1-R}$ $\quad$ R ≤ 0

$$R = \frac{K_{I,min}}{K_{I,max}}$$

C
BLESS VERSION 4.3 EQUATIONS

C.1 K1 Formulations per Zahoor 85 [11]

C.1.1 Full Circumference Internal Part-Through Crack

$$A = \{0.125(R_i/t) - 0.25\}^{0.25} \quad \text{for } 5 \le R_i/t \le 10$$
$$A = \{0.4(R_i/t) - 3.0\}^{0.25} \quad \text{for } 10 < R_i/t \le 20$$
$$F(R_i/t\,, a/t) = 1.1 + A\{1.948(a/t)^{1.5} + 0.3342(a/t)^{4.2}\}$$
$$K_1 = \sigma_t\sqrt{\pi a}F(R_i/t\,, a/t)$$

Where:

t = pipe wall thickness

R_i = piper inner radius

P = axial load

σ_t = $P/2\pi Rt$

R = $R_i + t$

C.1.2 Long Axial Part-Through Crack

$$A = \{0.125(R_i/t) - 0.25\}^{0.25} \quad \text{for } 5 \le R_i/t \le 10$$
$$A = \{0.4(R_i/t) - 1.0\}^{0.25} \quad \text{for } 10 < R_i/t \le 20$$
$$F(R_i/t\,, a/t) = 1.1 + A\{4.951(a/t)^2 + 1.092(a/t)^4\}$$
$$K_1 = \frac{2pR_o^2}{R_o^2 - R_i^2}\sqrt{\pi a}F(R_i/t\,, a/t)$$

Where:

R_o = pipe outer radius

P = internal pressure

Export Control Restrictions

Access to and use of EPRI Intellectual Property is granted with the specific understanding and requirement that responsibility for ensuring full compliance with all applicable U.S. and foreign export laws and regulations is being undertaken by you and your company. This includes an obligation to ensure that any individual receiving access hereunder who is not a U.S. citizen or permanent U.S. resident is permitted access under applicable U.S. and foreign export laws and regulations. In the event you are uncertain whether you or your company may lawfully obtain access to this EPRI Intellectual Property, you acknowledge that it is your obligation to consult with your company's legal counsel to determine whether this access is lawful. Although EPRI may make available on a case-by-case basis an informal assessment of the applicable U.S. export classification for specific EPRI Intellectual Property, you and your company acknowledge that this assessment is solely for informational purposes and not for reliance purposes. You and your company acknowledge that it is still the obligation of you and your company to make your own assessment of the applicable U.S. export classification and ensure compliance accordingly. You and your company understand and acknowledge your obligations to make a prompt report to EPRI and the appropriate authorities regarding any access to or use of EPRI Intellectual Property hereunder that may be in violation of applicable U.S. or foreign export laws or regulations.

The Electric Power Research Institute Inc., (EPRI, www.epri.com) conducts research and development relating to the generation, delivery and use of electricity for the benefit of the public. An independent, nonprofit organization, EPRI brings together its scientists and engineers as well as experts from academia and industry to help address challenges in electricity, including reliability, efficiency, health, safety and the environment. EPRI also provides technology, policy and economic analyses to drive long-range research and development planning, and supports research in emerging technologies. EPRI's members represent more than 90 percent of the electricity generated and delivered in the United States, and international participation extends to 40 countries. EPRI's principal offices and laboratories are located in Palo Alto, Calif.; Charlotte, N.C.; Knoxville, Tenn.; and Lenox, Mass.

Together…Shaping the Future of Electricity

1018999

Electric Power Research Institute
3420 Hillview Avenue, Palo Alto, California 94304-1338 • PO Box 10412, Palo Alto, California 94303-0813 • USA
800.313.3774 • 650.855.2121 • askepri@epri.com • www.epri.com